GEAP-4214

SODIUM COOLED REACTORS PROGRAM

FAST CERAMIC REACTOR DEVELOPMENT PROGRAM

Sixth Quarterly Report, January — March, 1963

Edited by
F. J. Leitz

April 1963

Atomic Power Equipment Department
General Electric Company
San Jose, California

UNITED STATES ATOMIC ENERGY COMMISSION • DIVISION OF TECHNICAL INFORMATION

LEGAL NOTICE

Printed in USA. Price $1.75. Available from the Office of Technical Services, Department of Commerce, Washington 25, D. C.

USAEC Division of Technical Information Extension, Oak Ridge, Tennessee

GEAP-4214
REACTOR TECHNOLOGY

SODIUM-COOLED REACTORS PROGRAM

FAST CERAMIC REACTOR DEVELOPMENT PROGRAM

Sixth Quarterly Report

January - March, 1963

Prepared for the
United States Atomic Energy Commission
Under
Contract No. AT(04-3)-189, Project Agreement No. 10

April 1963

ATOMIC POWER EQUIPMENT DEPARTMENT

GENERAL ELECTRIC

SAN JOSE, CALIFORNIA

TABLE OF CONTENTS

LIST OF ILLUSTRATIONS

LIST OF TABLES

SECTION I

INTRODUCTION

The Fast Ceramic Reactor Development Program is an integrated analytical and experimental program directed toward the development of fast reactors employing ceramic fuels, with particular attention to mixed plutonium-uranium oxide. Its major objectives are:

a. Development of a reliable, high performance fast reactor having nuclear characteristics which provide stable and safe operation, and

b. Demonstration of low fuel cycle cost capability for such a reactor, primarily through achieving high burnup of ceramic fuels operating at high specific power.

Progress during the period January 1 - March 31, 1963 on the currently active tasks of this program is described in subsequent sections.

This is the sixth in a series of quarterly progress reports written in partial fulfillment of Contract AT(04-3)-189, Project Agreement No. 10, between the United States Atomic Energy Commission and the General Electric Company. Prior progress reports to the Commission under this contract include the following:

Monthly Progress Letters, Nos. 1-41, from July 1959 through February 1963.

GEAP-3888 FCR Development Program - First Quarterly Report; October - December, 1961.

GEAP-3957 FCR Development Program - Second Quarterly Report, January - March, 1962

GEAP-3981 FCR Development Program - Third Quarterly Report, April - June, 1962.

GEAP-4080 FCR Development Program - Fourth Quarterly Report, July - September, 1962.

GEAP-4158 FCR Development Program - Fifth Quarterly Report, October - December, 1962.

Supplementary Progress Letters, Nos. 1-2, from October 1962 through January 1963, Reports from G. D. Collins and W. J. Ozeroff on assignment to CEA-France.

In addition, the following topical reports have been issued:

GEAP-3287 Fast Oxide Breeder - Reactor Physics, Part I - Parametric Study of 300 MWe Reactor Core, P. Greebler, P. Aline, J. Sueoka; November 10, 1959.

GEAP-3347 Fast Oxide Breeder - Stress Considerations in Fuel Rod Design. K. M. Horst; March 28, 1960.

GEAP-3486 Fast Oxide Breeder Project - Fuel Fabrication.
Part I - Plutonium-Uranium Dioxide Preparation and Pelletized Fuel Fabrication, J. M. Cleveland, W. C. Cavanaugh;
Part II - Fabrication of Plutonium-Uranium Dioxide Specimens by Swaging. M. E. Snyder, W. C. Cowden; August 15, 1960.

GEAP-3487 Fast Oxide Breeder - Preliminary Sintering Studies of Plutonium-Uranium Dioxide Pellets. J. M. Cleveland, W. C. Cavanaugh; August 15, 1960.

GEAP-3646 Calculation of Doppler Coefficient and Other Safety Parameters for a Large Fast Oxide Reactor. P. Greebler, B. A. Hutchins, J. R. Sueoka; March 9, 1961.

GEAP-3721 Core Design Study for a 500 MWe Fast Oxide Reactor. K. M. Horst, B. A. Hutchins, F. J. Leitz, B. Wolfe; December 28, 1961.

GEAP-3824 Fabrication Cost Estimate for UO_2 and Mixed PuO_2 Fuel. G. D. Collins; January 24, 1962.

GEAP-3833 The Post-Irradiation Examination of a PuO_2-UO_2 Fast Reactor Fuel, J. M. Gerhart; November 1961.

GEAP-3856 Experimental Fast Oxide Reactor, K. P. Cohen, M. J. McNelly, B. Wolfe; November 27, 1961.

GEAP-3876 Plutonium Fuel Processing and Fabrication for Fast Ceramic Reactors, H. W. Alter, G. D. Collins, E. L. Zebroski; February 1, 1962.

GEAP-3880 Comparative Study of PuC-UC and PuO_2-UO_2 as Fast Reactor Fuel, Part I - Technical Considerations, K. M. Horst, B. A. Hutchins; February 15, 1962. Part II - Economic Considerations, G. D. Collins; November 15, 1962.

GEAP-3885 Experimental Fast Ceramic Reactor Design. Status Report as of October 31, 1961. Edited by K. M. Horst; April 24, 1962.

GEAP-3923 Resonance Integral Calculations for Evaluation of Doppler Coefficients - The RAPTURE Code, J. H. Ferziger, P. Greebler, M. D. Kelley, J. Walton; June 12, 1962.

GEAP-4028 A Fuel Reprocessing Plant for Fast Ceramic Reactors, H. W. Alter; February 1, 1962.

GEAP-4058 Analytical Studies of Transient Effects in Fast Reactor Fuels, R. B. Osborn and D. B. Sherer; August, 1962.

GEAP-4090 FORE - A Computational Program for the Analysis of Fast Reactor Excursions, P. Greebler, D. B. Sherer; October, 1962.

GEAP-4130 Experimental Studies of Transient Effects in Fast Reactor Fuels, Series I, UO_2 Irradiations, J. H. Field; November 15, 1962.

GEAP-4092 Doppler Calculations for Large Fast Ceramic Reactors, Effects of Improved Methods and Recent Cross-Section Information, P. Greebler, E. Goldman; December, 1962.

SECTION II

SUMMARY

2.1 Task B - Vented Fuel Development

Three capsules containing mixed oxide fuel specimens have been fabricated for the second series of sodium logging tests. The nondefected control has been irradiated (eight 30 minute cycles at 25±2 kw/ft) and its examination is in progress. One of the fuel specimens in the remaining two capsules is defected, with a meltable silver solder plug in the defect; the other contains sodium in the cored center of the fuel and has no defect in the cladding for sodium escape.

Microstructure examination of the fuel in the Series I sodium logging specimens indicated localized Na-UO_2 reaction and also provided a basis for estimating central fuel temperature. The central temperature thus estimated confirmed the expected increase in effective thermal conductivity of the fuel due to sodium.

UO_2, PuO_2, and mixed oxide fuel pellets crumbled on static exposure to sodium at 650 C for 20 hours, with the exception of the pellet consisting of 20 percent PuO_2-UO_2 with an O/M ratio of 1.97. Swaged and pelleted mixed oxide fuel previously irradiated in Phase I appeared relatively stable on similar exposure to hot sodium, except that the stainless steel cladding on the swaged fuel sections cracked.

Design of capsules is proceeding for the investigation of fission product release to sodium and fission product plugging within the fuel.

2.2 Task C - Fuel Testing in TREAT

Following a preliminary irradiation at 40 percent of the goal energy pulse, capsule II-A, the first capsule containing a 0.25 inch diameter mixed oxide fuel specimen, successfully withstood transient irradiation which raised the peak fuel temperature to a calculated temperature of ~4900 F plus a small portion of the heat of fusion. Good agreement was obtained between burnup measured by gamma radiation and a revised calculation of the transient energy pulse. No measurable changes in fuel clad had occurred, and only slight bowing of the unrestrained specimen was observed. Preliminary internal examination revealed extensive radial fuel cracking and substantial reduction in the fuel-clad gap, but no central void formation.

2.3 Task E - Fuel Performance Evaluation

Preliminary capsule designs have been completed for (a) central fuel temperature measurement using gas thermometry and W-Re thermocouples, (b) high burnup irradiation tests of mixed

oxide fuel with O/M stoichiometry of 1.97, 2.00, and 2.04, and (c) plutonium migration investigation using plutonium-242 tracer.

A gravimetric method for determining O/M ratio of mixed oxide fuel has been developed and is being applied to test fuel samples. The method entails conversion of oxidized fuel to the stoichiometric O/M value of 2.000 by heating in dry 6 percent H_2-He gas at 700 C to constant weight. Apparatus for determining the melting point and x-ray structure of mixed oxide fuel has been installed and checked out.

Tap density and acid dissolution characteristics of mixed oxide powder have been determined over the entire range of plutonium/uranium composition.

2.4 Task F - Fast Flux Irradiation of Fuel

Efforts directed toward irradiation of mixed oxide fuel in EBR II have been reactivated, with scheduled delivery of a 19 encapsulated pin assembly to EBR II in November, 1963. Fuel pellets and clad parts for the first two fuel specimens have been fabricated. Conceptual design of the fuel specimens, capsules and hex tube assembly is complete and detailed design is in progress.

The alternate possibility of simulating fast flux irradiations in an ATR loop appears unpromising from both a cost and schedule standpoint.

2.5 Task G - Reactor Dynamics and Design

Calculation of the physics parameters for a ~1000 MWe FCR with a very low core H/D has been performed. For the case considered, such "pancaking" improved the sodium loss reactivity effect only slightly, at the expense of considerable reduction in the Doppler effect. Alternate core design modifications are under evaluation.

Using tne FORE code, a quantitative assessment has been made of the time provided by the Doppler effect to scram the reactor without core damage as a function of the magnitude and rate of accidental reactivity insertion.

Multilevel methods are being applied to calculate the effect of level interference on Pu-239 cross sections and, relatedly, on the Doppler coefficient. Computer code development in progress includes the generation of multigroup cross section files and modification to MISY, the diffusion theory code used for fast reactor analysis.

SECTION III

TASK B - VENTED FUEL DEVELOPMENT

3.1 Sodium Logging

3.1.1 Series I - UO_2 Fuel

The observed effects of the Series 1 sodium logging experiments performed to-date have been promising. As previously reported, no cladding damage has been observed after cycling the linear power of defected UO_2 specimens from 0 to 26 kw/ft, and after a single cycle from 0 to 22 kw/ft of a non-defected UO_2 specimen which had been fabricated to contain sodium in its cored center. However, evidence of some internal interaction between the sodium and the fuel has been detected which did not manifest itself as cladding damage. Investigation of the grain structure of the Series I specimens has been continued and is reported under the Sodium-Fuel Compatibility subtask (Section 3.2.1).

In the course of this preliminary evaluation, the central temperatures have been estimated by microstructure analysis (see Table III-2), assuming grain growth occurs at the same temperature in UO_2 as in sodium logged UO_2. Estimated temperature values determined in this manner indicate that these specimens operated at significantly cooler temperatures than the control specimen. Likewise, these calculations show general agreement with preliminary heat transfer calculations which assume that the pellet-to-clad gap is filled with sodium and a thermal conductivity value increased to 3.3 Btu/hr-ft-F for the fuel-sodium mixture. The sodium vapor pressures, corresponding to these central fuel temperatures, estimated from an extrapolation of available data, permit an estimation of maximum possible sodium vapor pressures within the fuel. These values are shown in Table III-1.

TABLE III - 1
MAXIMUM VAPOR PRESSURE ESTIMATES

Capsule	Linear Power (w/cm)	Estimated Central Temp (t_c) (°C)	Estimated Na Vapor Pressure at t_c [a] (atm)	Clad Burst [b] Pressure (atm)
B-I-A [c]	690	2600	- [c]	160
B-I-B,C,D [d]	660-760	1800	100	160
B-I-E [d]	850	2100	220	160
B-I-F [e]	720	2000	170	160

(a) Vapor pressure data extrapolated to critical point (Liquid Metals Handbook, Sodium NaK Supplement).

(b) Calculated burst pressure for 0.25 inch OD by 0.006 inch thick, 347 SS clad at 1200 F. The 0.2 percent yield point is 60 atm.

(c) Control sample without sodium inside cladding. The equivalent sodium vapor pressure is 500 atm.

(d) Defected samples.

(e) No defect, sodium in cored center of fuel.

As indicated in the table, specimens B, C, and D would not be expected to generate vapor pressures adequate to burst the clad even if the central fuel temperature is assumed as the effective temperature of the sodium, and it is also assumed that the vapor could not escape the clad through the defect. Specimen B-I-F is a special case because the sodium was fabricated in the center of the fuel and the capsule was given a single fast insertion into the test reactor flux where it was held for over one hour. Thus, the effective pressure in this case may have been dependent on the time required for the sodium to melt and redistribute into the pellet-to-clad gap and fuel open spaces. It is evident from the table that the final condition was not adequate to rupture the cladding, nor did it yield. Specimen B-I-E also did not burst nor yield the cladding and thus that either the defect was adequate to relieve the pressure or that the effective pressure was not equivalent to the central temperature. The same observation concerning the effective temperature is true for the other defected specimens (B, C, D) because the calculated 0.2 percent yield point of 60 atm would be exceeded by the sodium vapor pressure equivalent to the central temperature, yet deformation did not occur. The conclusion is that central fuel temperatures are not only significantly lower when sodium is inside the clad, but also central temperature is not the effective temperature insofar as the sodium vapor pressure exerted on the cladding.

3.1.2 Series II - Mixed PuO_2-UO_2 Fuel

A second series of sodium logging capsules have been designed, fabricated and irradiation initiated to investigate the sodium logging characteristics of mixed oxide fuel. During the report period, three capsules were fabricated and the non-defected control sample (B-II-A) was

irradiated during peak flux conditions of GETR cycle 41. The irradiation consisted of eight 30 minute cycles at a linear power generation rate of 25 ± 2 kw/ft. The RML examination has begun but results are not yet available.

Capsule B-II-B is identical to B-II-A except that the fuel has been core-drilled and filled with sodium similar to Series I specimen B-I-F. However, the volume of void spaces available for sodium to distill to have been reduced. Capsule B- II-C is identical to B-II-A except this specimen has been intentionally defected. Capsule B-II-C will be given 100 short irradiation cycles. The defect hole is sealed with a meltable plug of silver solder which permitted fabrication of this specimen using the standard procedure. Specimens B-II-B and B-II-C will be irradiated during peak flux conditions of GETR cycle 43 in April, 1963.

3.2 Sodium-Fuel Compatibility

3.2.1 Sodium Logging Specimen Examinations (UO_2)

Hot cell examinations of the Series I sodium logging capsules were continued during this period. Table III-2 reviews the capsule parameters and the observations on the fuel microstructure after sodium logging. The results of the sodium logging experiments were reported previously. The microstructure analysis indicate that a reaction has occurred between UO_2 and sodium plus sodium oxide in the sodium logging specimens. The suspected reaction zones in specimens B-I-F and B-I-E are noted in Figures 3-1 and 3-2. Figure 3-3 shows the fuel microstructure of the reference capsule B-I-A.

The reaction in specimen B-I-F is of interest because of the apparent preferential attack near the outer edges of the fuel. As previously stated, the sodium evidently redistributed from the central core into the gap and fuel void spaces in the affected outer zone of the fuel. Since this specimen was not cycled, the sodium and sodium oxide probably remained in this zone throughout the irradiation at temperatures from about 1200 to 1500 F.

Center temperature calculations on the Na-logging experiments indicated that center melting did not occur in any of the capsules. In fact, the capsules with sodium present in the annulus and in the open porosity exhibited significantly lower center temperatures because of the extremely high gap conductance and, evidently, higher effective fuel conductivity afforded by the sodium. Table III-3 lists a summary of the center temperature experienced by the Na-logging capsules as determined by microstructure studies. These calculations are based on integrated thermal conductivity values for UO_2 and thus represent the highest probable values of central temperature.

Although of no specific interest to sodium-fuel compatability, the reference capsule B-I-A (Figure 3-3) shows an interesting UO_2 microstructure. The UO_2 fuel pellets in this experiment were inadvertently fabricated with a semi-triangular shape resulting in uneven gap

TABLE III-2

EVIDENCE FOR Na-UO_2 REACTION IN
SERIES I Na-LOGGING CAPSULE IRRADIATIONS

Capsule Number	Fuel Rod Power kw/ft	Defect Diameter (in.)	Fuel Clad Surface Temperature °F	Thermal Cycles	Time At Full Power hrs	Microstructure Observations
B-I-A	21	None	1080	5	4.5	Control sample.
B-I-B	23	0.005	1135	7	3.5	No significant microstructure change due to Na-UO_2 reaction.
B-I-C	22	0.005	1090	7	3.5	Possible reaction zone.
B-I-D	20	0.005	1015	8	4.0	Distinct reaction zone throughout fuel cross section.
B-I-E	26	0.005	1240	8	4.0	Probable reaction area in fuel center.
B-I-F	22	None[a]	1030	1	1.17	Distinct reaction zone adjacent to clad - possible reaction area in fuel center.

(a) Sodium fabricated in void before in-pile testing.

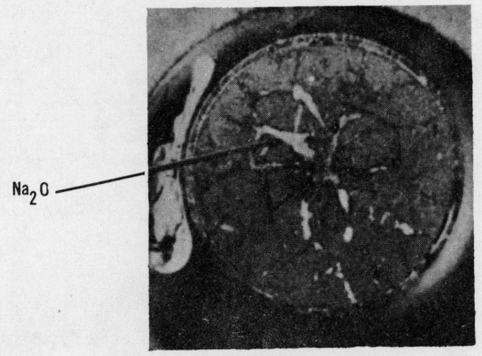

10X

PHOTOMACROGRAPH OF FUEL CROSS SECTION
PRIOR TO CLEANING WITH ALCOHOL

10X

PHOTOMACROGRAPH OF FUEL CROSS SECTION
AFTER CLEANING WITH ALCOHOL

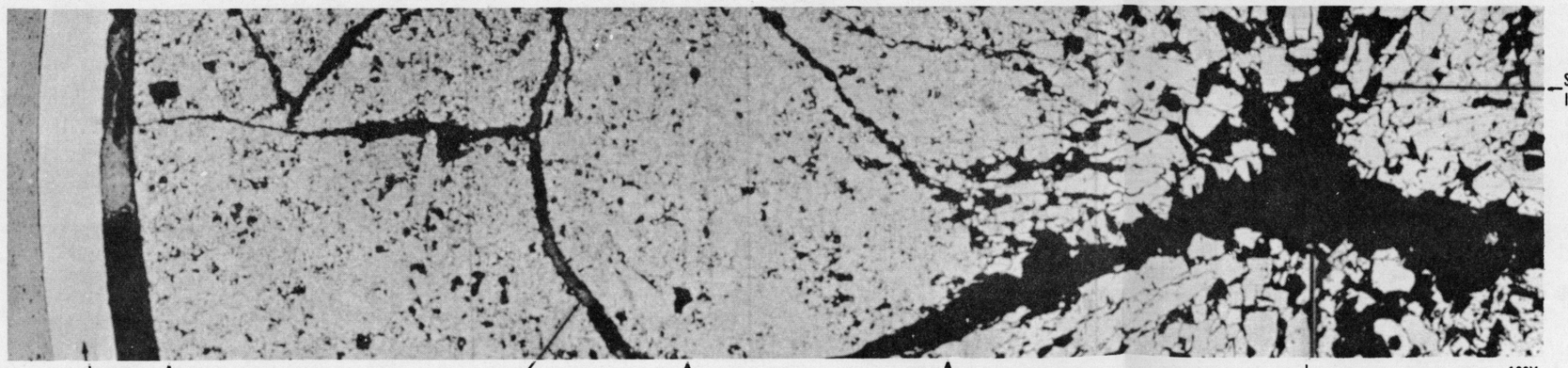

Figure 3-1. Photomicrographs of UO_2 Cross Section From Capsule B-1-E

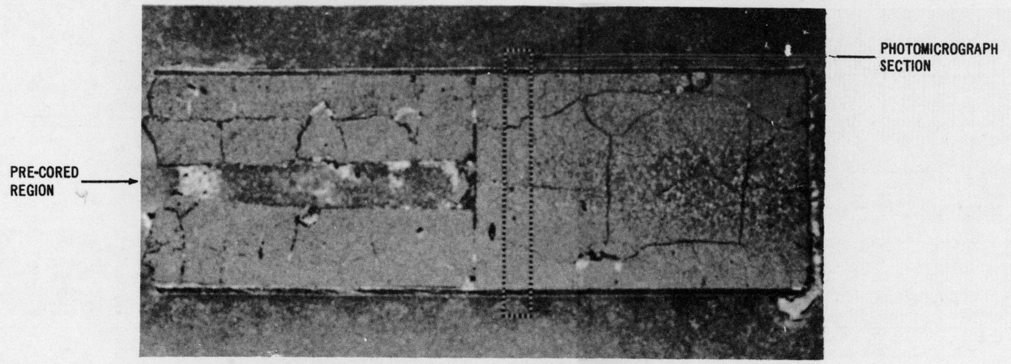

PHOTOMACROGRAPH OF POLISHED FUEL SECTION

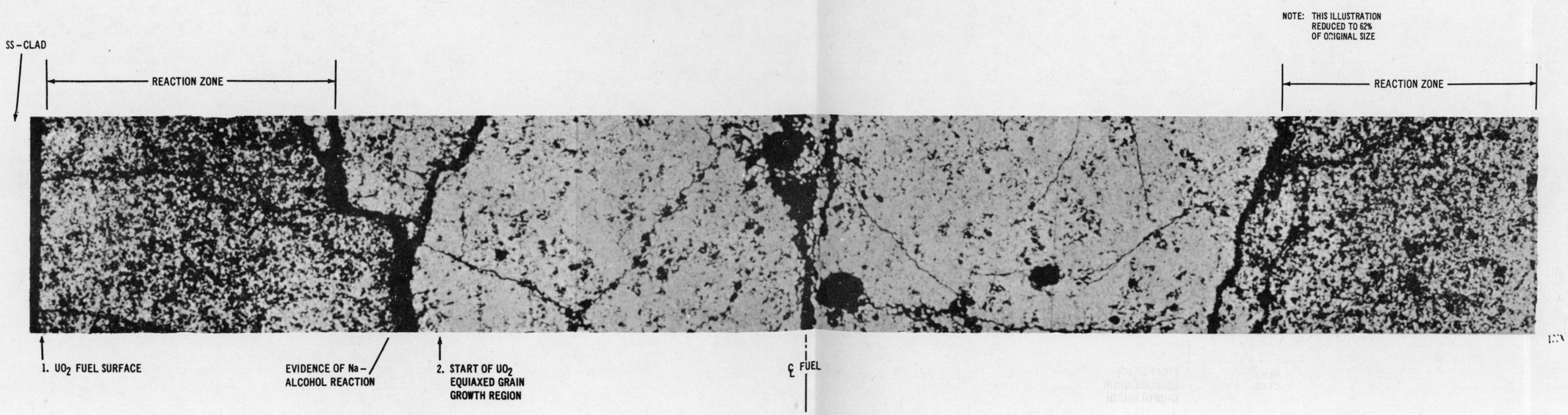

NOTE: THIS ILLUSTRATION REDUCED TO 62% OF ORIGINAL SIZE

Figure 3-2. Photomicrographs of UO_2 Cross Section from Capsule B-1-F (Top Section)

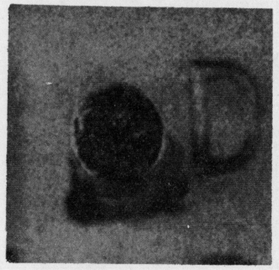

2X

PHOTOMACROGRAPH OF FUEL
CROSS-SECTION

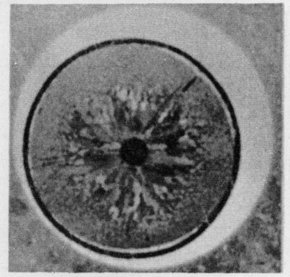

10X

PHOTOMACROGRAPH OF POLISHED
FUEL CROSS-SECTION

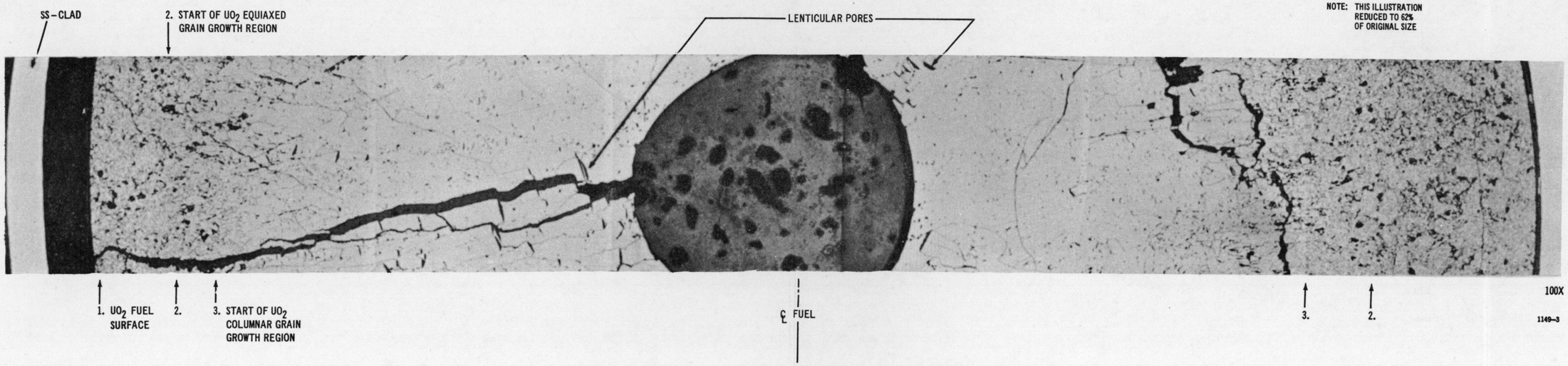

Figure 3-3. Photomicrographs of UO_2 Cross Section from Capsule B-1-A

TABLE III - 3

ESTIMATE OF FUEL CENTER TEMPERATURES IN SERIES I Na-LOGGING FUEL CAPSULES

Capsule No.	Fuel Rod Power Level w/cm	Fuel Clad Surface Temperature °C	$\int_{T_s}^{T_c} k d\theta$ w cm	$\int_{0}^{T_s} k d\theta$ w cm	$\int_{0}^{T_c} k d\theta$ w cm	Center Temperature Estimates Based on AECL Data (a) °C	Grain Growth Observations
B-I-A	690	585	46	37	83	2600	Massive columnar grain growth
B-I-B	760	610	20	-	-	1800	Little or no grain growth
B-I-C	720	590	48	-	-	1800	Little or no grain growth
B-I-D	660	550	44	-	-	1600	Little or no grain growth
B-I-E	850	670	57	11	68	2100	Slight columnar grain growth
B-I-F (b)	720	560	48	15	63	2000 (b)	Slight columnar grain growth

(a) A. S. Bain, et al, "UO_2 Irradiations of Short Duration", Part II, AECL-1192.

(b) The pellet analyzed is the top uncored pellet which was operated at a somewhat higher power than the average stated.

conductance (see Figure 3-3). Because of this variable conductance, the fuel microscructure exhibits a dual structure. The areas with high gap conductance have unusually large equiaxed grains along with incipient lenticular pores. The areas with low gap conductance on the other hand contain lenticular pores caught in the process of sweeping the thermal gradient, thereby forming columnar grains.

3.2.2 Static Na-UO_2

The static Na-UO_2 compatibility test program has been delayed due to scheduling problems in fabricating the UO_2 pellets. Present plans call for studies to determine the effect of time, temperature, O/U ratio, and Na_2O content on Na-UO_2 compatibility. A second series of tests will be initiated on UO_2-20 percent PuO_2 if the static tests on UO_2 give reproducible results. Preliminary static tests on UO_2-Na compatibility have shown that the UO_2 density is a critical parameter. Table III-4 summarizes the results from these tests. Based on microstructure comparison, the attack on samples 7 and 8 of Table III-4 resembles that observed in the sodium logging specimens.

3.2.3 Mixed PuO_2-UO_2

Preliminary tests using static capsules to explore the compatibility of sodium and unirradiated mixed oxide fuel pellets have been completed. The exposure time was 20 hours at 650 C. Only one of five pellets survived the test without significant change in weight or dimensions. This pellet was of FCR reference composition (20 percent PuO_2 -80 percent UO_2) with an oxygen-to-metal ratio of 1.97 0.02. The other pellets were observed to have severely crumbled during the test. The test results are summarized in Table III-5.

Also during the report period, four sections were selected from FCR Phase I irradiated mixed PuO_2-UO_2 specimens, as listed in Table III-6, and heated in capsules filled with sodium.

The sections of irradiated fuel included cladding and thus the fuel was exposed to sodium at both ends. Each fuel section was heated at 650 C for a total of 20 hours, with cycling to room temperature a total of three times during this period. After this treatment the fuel meat appeared to be intact, but the cladding on both swaged specimens had grossly fractured. Metallographic examination of these samples is continuing to determine the nature of these clad fractures, and also to determine if fuel crystal structure damage has resulted from contact with the sodium or sodium oxide.

Since these capsules were originally bathed in NaK during their irradiation over two years ago (after which no external surface cracks were evidenced) and since they have been stored in air since that time, caustic stress corrosion cracking during storage is the suspected cause for the observed fracture.

TABLE III-4

PRELIMINARY STATIC Na-UO_2 COMPATIBILITY TESTS

Sample No.	Density %Theor.	Na(a) Temperature C	Exposure(b) Time hrs	O U Ratio Pre	Weight, gms.			Pellet Condition - Post
					Pre	Post	Post-Pre	
1	78	540	1 hr	2.01	~30.	-	-	Disintegrated
2	78	540	1 hr	2.06	~30.	-	-	Disintegrated
3	79	540	1 hr	2.00	~30.	-	-	Disintegrated
4	80	540	1 hr	2.06	~30.	-	-	Disintegrated
5	80	540	1 hr	2.00	~30.	-	-	Disintegrated
6	82	540	1 hr	2.01	~30.	-	-	Disintegrated
7	90	428	6 hrs	2.01	3.0487	Not avail.	Not avail.	Serious surface pitting
8	90.5	570	6 hrs	2.01	2.2650	Not avail.	Not avail.	Serious surface pitting
9	91.0	428	6 hrs	2.01	2.2826	Not avail.	Not avail.	No attack
10	91.5	570	6 hrs	2.01	3.0596	Not avail.	Not avail.	Slight surface attack
11	95	570	5.5 hrs	2.00	30.55	30.56	+0.01	No attack
12	96	540	1 hr	2.00	38.489	38.483	-0.005	No attack
13	96	540	1 hr	2.01	39.004	39.001	-0.003	No attack
14	97	540	4	2.01	39.300	39.300	0	No attack
15	97	540	3	2.01	38.373	38.355	-0.028	No attack

(a) Specimen inserted in sodium at 70 C, then heated to tabulated temperature in 60-90 minutes.

(b) Time at maximum temperature, exclusive of heating interval

TABLE III - 5

SODIUM-FUEL COMPATIBILITY TESTS

Capsule	Pellet Nominal Composition	O M Ratio(a)	Density (g cc)	Diameter (in)	Length (in)	Weight (g)	Test Results[b]
1	UO_2	2.00	9.67	0.2184-0.2186	0.3770	2.2403	Specimen was crumbled.
2	20% PuO_2-80% UO_2	1.97	10.56	0.2190-0.2191	0.2440	1.5963	Specimen not significantly changed Diameter 0.2190-0.2200 Weight 1.5972 g
3	20% PuO_2-80% UO_2	2.04	10.54	0.2179-0.2198	0.2502	1.6270	Specimen was crumbled.
4	28% PuO_2-72% UO_2	1.96	10.43	0.2178	0.2572	1.6674	Specimen was crumbled.
5	PuO_2	1.65	9.89	0.2110-0.2111	0.2778	1.5909	Specimen was reduced to powder

(a) O/M ratio estimated from analysis of similar pellet.

(b) Exposure was for an accumulated 20 hours at 650 ± 20 C obtained in four to eight hour periods.
Approximately one gram of sodium was in each capsule.
Sodium removal was by dissolving in mercury over a two-week period.

TABLE III - 6
PHASE I FUEL SPECIMEN CHARACTERISTICS

Specimen	Burnup (MWD/T)	Average Heat Flux, Btu/hr-ft^2	Central Void Diameter, In.	Pre-Irradiation Density (% Theoretical)
VII-1-Swaged	70.300	1.31×10^6	0.051 - 0.060	~75
VI-4-Swaged	30.900	0.62×10^6	0 - 0.026	~75
IX-2-Pelleted	38.300	1.19×10^6	0.022 - 0.031	94.8
VI-3-Pelleted	34.900	0.76×10^6	0 - 0.031	92.3

These sections were selected to cover a range of fabrication technique, burnup and heat flux.

3.3 Fission Product Plugging

Detailed design is continuing of two capsule experiments (see GEAP-4158) intended to proof-test the vented-through-blanket design of vented fuel elements. Physics, heat transfer, and mechanical design calculations have been completed and comment drawings of the final concept issued. The AEC Form 21 has also been submitted for approval.

One of the unique features of the design is the incorporation in one of the capsules of a thermostating device to conduct heat from the power-generating portion of the capsule up to the blanket region. Thus, the need for heaters is eliminated.

Another feature which is currently being designed along with the capsule is continuous pressure monitoring equipment to record the fission gas pressure buildup in the reservoir.

3.4 Fission Product Release

Three capsules have been designed to study the release of fission products from mixed oxide fuel into static sodium. During the period, approved drawings have been issued and Form 21 approvals requested.

The concept of three capsules stacked into a single assembly, described last quarter, has been discarded in favor of three single capsules. Two of the capsules include fuel specimens designed to release gaseous and volatile fission products to the sodium. The third specimen simulates a fuel rod which has failed by rupture of the cladding. Figure 3-4 illustrates the fuel rod designs. Specimen B-IV-A has a 1-13 16-inch long UO_2 blanket above the fuel and the fission gases must pass through the UO_2 to the top vent. Specimen B-IV-B is bottom vented and the UO_2 is limited to that required for thermal insulation of the end cap weld. Specimen B-IV-C has no vent but is defected with a 0.005-inch hole located near the midpoint.

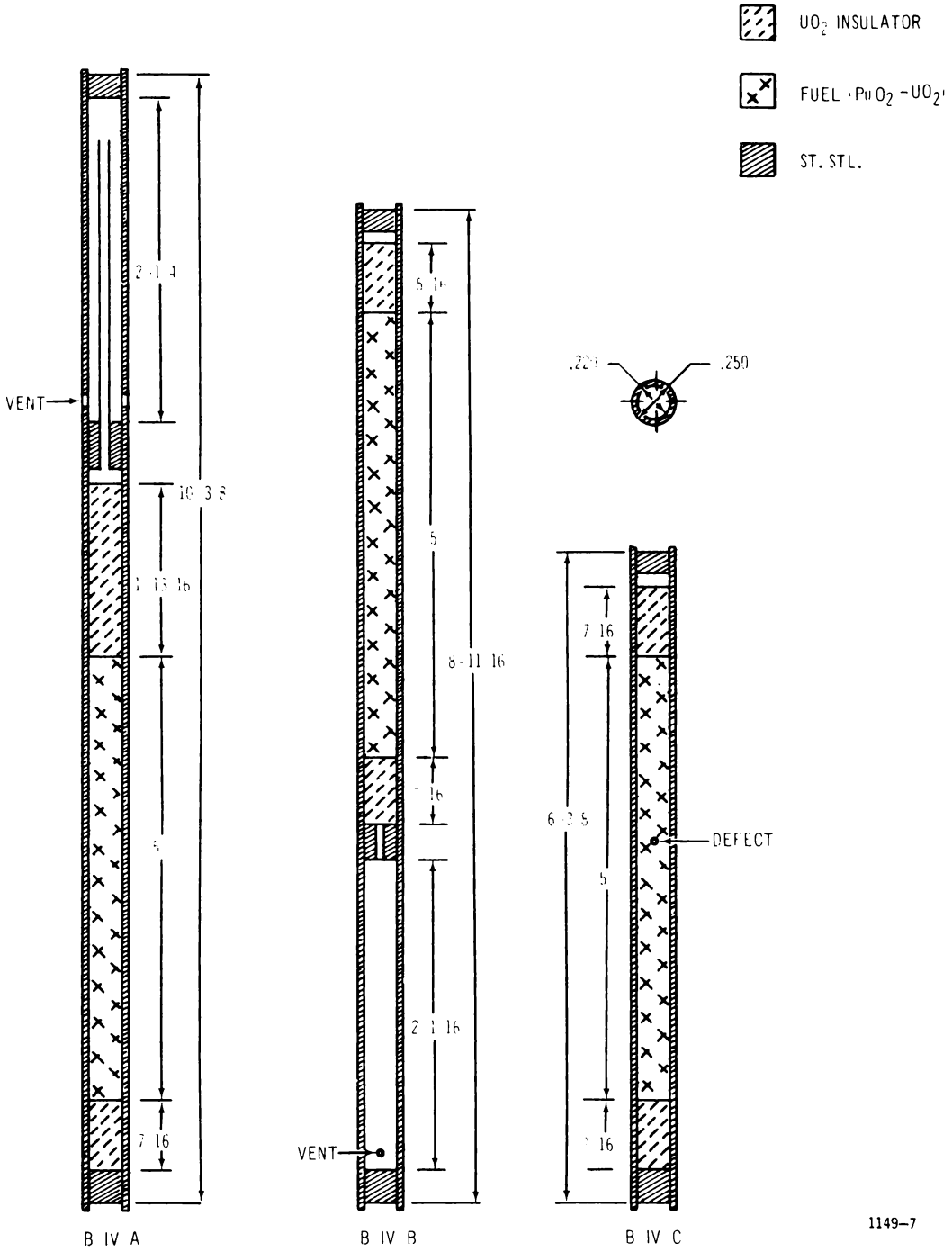

Figure 3-4. Fission Product Release Fuel Specimens

The capsule design is shown in Figure 3-5. All capsules are double-contained and are instrumented with thermocouples in the sodium annulus around the fuel specimen, as well as the NaK annulus around the sodium container. Thermocouples for calorimetric measurement of capsule power are also provided in the coolant channel.

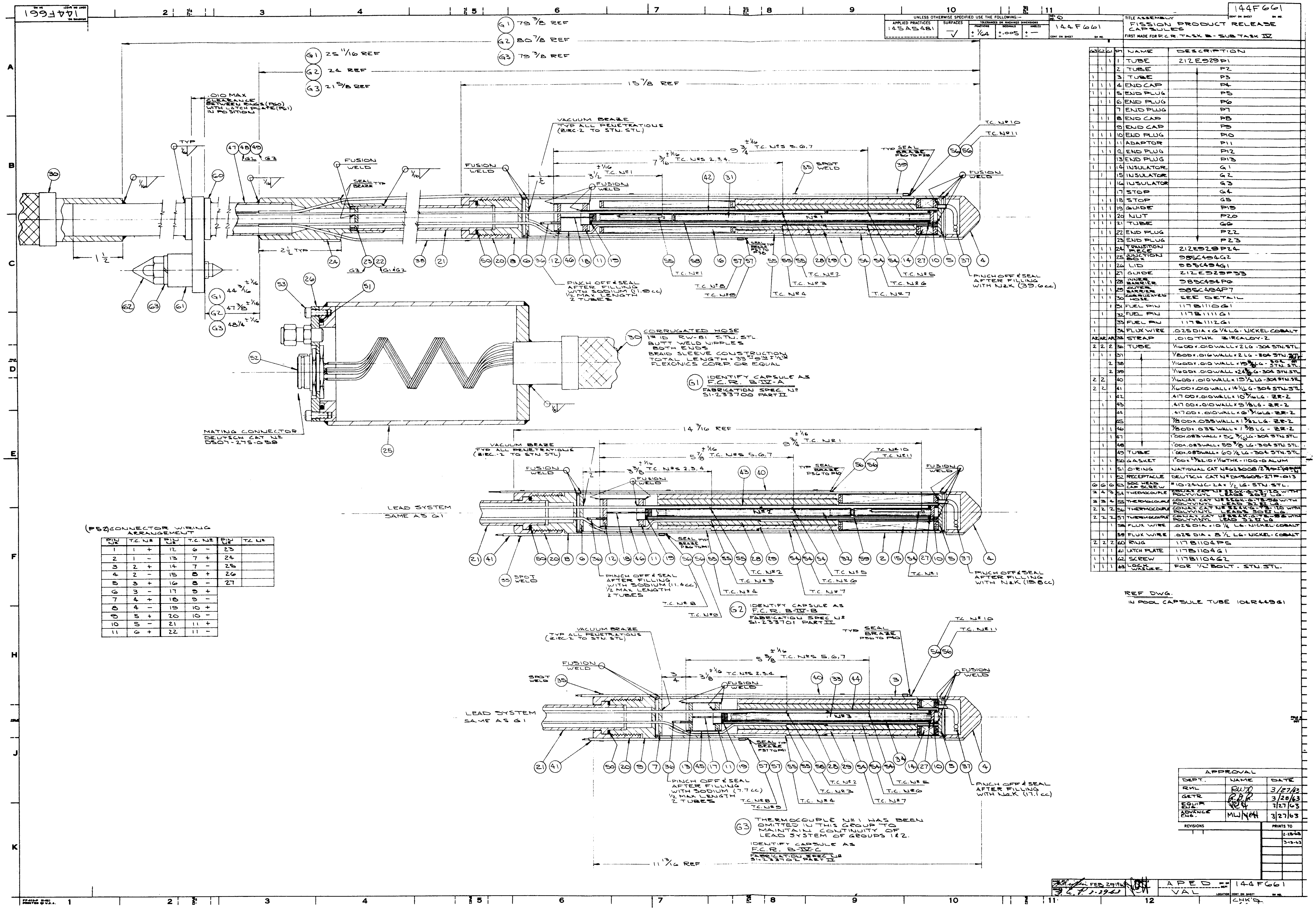

G3	G2	G1	PT	NAME	DESCRIPTION
		1	1	TUBE	212E929P1
	1		2	TUBE	P2
1			3	TUBE	P3
1	1	1	4	END CAP	P4
1	1	1	5	END PLUG	P5
	1	1	6	END PLUG	P6
1			7	END PLUG	P7
	1	1	8	END CAP	P8
1			9	END CAP	P9
1	1	1	10	END PLUG	P10
1	1	1	11	ADAPTOR	P11
	1	1	12	END PLUG	P12
1			13	END PLUG	P13
1		1	14	INSULATOR	G1
	1		15	INSULATOR	G2
		1	16	INSULATOR	G3
1			17	STOP	G4
	1	1	18	STOP	G5
1	1	1	19	GUIDE	P19
1	1	1	20	NUT	P20
1	1	1	21	TUBE	G6
	1	1	22	END PLUG	P22
1			23	END PLUG	P23
1	1	1	24	TRANSITION PIECE	212E929P24
1	1	1	25	JUNCTION BOX	985C494G2
1	1	1	26	LID	985C494G1
1	1	1	27	GUIDE	212E929P33
1	1	1	28	INNER BARRIER	985C494P6
1	1	1	29	OUTER BARRIER	985C494P7
1	1	1	30	CORRUGATED HOSE	SEE DETAIL
		1	31	FUEL PIN	117B1110G1
	1		32	FUEL PIN	117B1111G1
1			33	FUEL PIN	117B1112G1
1			34	FLUX WIRE	.025 DIA x 6 1/4 LG - NICKEL-COBALT
AR	AR	AR	35	STRAP	.010 THK ZIRCALOY-2
2	2	2	36	TUBE	1/16 OD x .010 WALL x 2 LG - 304 STN. STL.
1	1	1	37		1/8 OD x .016 WALL x 2 LG - 304 STN. STL.
		2	38		1/16 OD x .010 WALL x 15 5/8 LG - 304 STN. STL.
		2	39		1/16 OD x .010 WALL x 24 1/8 LG - 304 STN. STL.
2	2		40		1/16 OD x .010 WALL x 19 1/2 LG - 304 STN. STL.
2	2		41		1/16 OD x .010 WALL x 14 1/2 LG - 304 STN. STL.
		1	42		.417 OD x .010 WALL x 10 15/16 LG - ZR-2
	1		43		.417 OD x .010 WALL x 9 1/8 LG - ZR-2
1			44		.417 OD x .010 WALL x 6 13/16 LG - ZR-2
1			45		7/8 OD x .035 WALL x 1 5/32 LG - ZR-2
	1	1	46		7/8 OD x .035 WALL x 1 3/8 LG - ZR-2
		1	47		1" OD x .083 WALL x 56 3/16 LG - 304 STN STL
	1		48		1" OD x .083 WALL x 59 3/8 LG - 304 STN. STL.
1			49	TUBE	1" OD x .083 WALL x 60 1/4 LG - 304 STN. STL.
1	1	1	50	GASKET	1" OD x 23/32 ID x 1/16 THK - 1100-0 ALUM
1	1	1	51	O-RING	NATIONAL CAT NO 623008 (2 ¼ OD x 2 1/4 ID) BUNA-N
1	1	1	52	RECEPTACLE	DEUTSCH CAT NO DM5605-27P-013
6	6	6	53	SOC HEAD CAP SCREW	#10-24 UC-2A x 1/2 LG - STN. STL.
3	4	3	54	THERMOCOUPLE	CONAX CAT NO 556K-6-T3-120 WITH POLYVINYL LEADS 30 FT LG.
3	3	4	55	THERMOCOUPLE	CONAX CAT NO 556K-6-T3-56 WITH POLYVINYL LEAD 32 FT LG.
2	2	2	56	THERMOCOUPLE	CONAX CAT NO 554K-6-T3-120 WITH POLYVINYL LEADS 30 FT LG.
2	2	2	57	THERMOCOUPLE	CONAX CAT NO 554K-6-T3-56 WITH POLYVINYL LEAD 32 FT LG
		1	58	FLUX WIRE	.025 DIA x 10 1/4 LG - NICKEL-COBALT
	1		59	FLUX WIRE	.025 DIA x 8 1/2 LG - NICKEL-COBALT
2	2	2	60	RING	117B1104P5
1	1	1	61	LATCH PLATE	117B1104G1
1	1	1	62	SCREW	117B1104G2
1	1	1	63	LOCK WASHER	FOR 1/2" BOLT - STN. STL.

(P52) CONNECTOR WIRING ARRANGEMENT

PIN NO	T.C. NO		PIN NO	T.C. NO		PIN NO	T.C. NO
1	1	+	12	6	-	23	
2	1	-	13	7	+	24	
3	2	+	14	7	-	25	
4	2	-	15	8	+	26	
5	3	+	16	8	-	27	
6	3	-	17	9	+		
7	4	+	18	9	-		
8	4	-	19	10	+		
9	5	+	20	10	-		
10	5	-	21	11	+		
11	6	+	22	11	-		

Figure 3-5. Fission Product Release Capsules

SECTION IV

TASK C - FUEL TESTING IN TREAT

4.1 Series I Tests

Series I testing of 1.0 inch diameter, UO_2 fueled specimens has been completed and distribution has been made of a topical report [1] discussing the results and conclusions thereof. Further non-destructive metallographic examination of specimen I-D (~7000 F estimated peak fuel temperature, with extensive central void and vapor bubble formation) will be undertaken by the Hanford Laboratories Operation to study the kinetics of grain growth.

4.2 Series II Tests

The initial transient irradiation of a 0.25 inch diameter, mixed oxide (20 percent PuO_2-UO_2) fuel specimen was accomplished during this quarter. The first transient on capsule II-A was a 60 MWsec pulse initiated on a 0.313 sec period with a 0.96 percent ΔK reactivity insertion. Analysis of the test data indicated that the 60 MWsec transient run resulted in a capsule equilibrium temperature rise of only ~96 F instead of the 258 F expected (275 F for 64 MWS originally estimated). This indicated a total sample power of 21.5 Btu for the transient. Resolution of this discrepancy was based upon two possibilities: (a) higher capsule heat capacity than previously calculated or (b) lower than predicted sample power generation. Calculations, assumptions, and capsule design criteria were reviewed in an effort to determine which of these factors was responsible for the discrepancy.

Findings indicated that this apparent factor of 2.7 between planned and experimental results was explained by a combination of corrections to heat capacity and physics computations.

4.2.1 Heat Capacity Calculations

A review of the physical model used in the original heat transfer computer calculations revealed that a total capsule heat capacity of 0.189 Btu F was utilized to give an equilibrium temperature rise of 275 F for a 64 MWsec transient. A recalculation of the capsule heat capacity (with a revision to the quantity of NaK included) and attempts to reconcile measured calibration values indicated that the effective total capsule heat capacity could be as high as 0.224 Btu/F during the time required (~30 sec) to reach the capsule equilibrium temperature (96 F measured).

It was assumed that the outer capsule (heater can and shroud tube) did not rise in temperature during the initial 30 sec of the transient, and that only the 11 inch length of the inner capsule contacted by NaK was involved. The results of this recalculation using the average temperatures indicated in the first transient are given as follows:

	Weight	Average Temperature	Cp. (Btu # F)	Btu F
Aluminum	0.379 #	(875 F)	0.26	0.0985
Stainless-Steel				
Clad	0.032 #	(950 F)	0.138	0.0045
Capsule tube	0.484 #	(825 F)	0.140	0.0677
Remainder (end plugs, etc.)	0.150 #	(850 F)	0.140	0.0210
Fuel	0.1034#	(2000 F)	0.0785	0.0081
NaK	0.1045#	(875 F)	0.210	0.0220
Thermoflex	0.006 #	(850 F)	0.35	0.0021
			Total	0.224 Btu F

It was recognized that this recalculated value was based upon an assumption of the amount of capsule which heats up during a 30 sec transient interval. However, it was felt that a good approximation was chosen and this error should be small. Thus, review of computer calculations and revisions to the heat capacity accounted for a factor of approximately 1.2.

4.2.2 Physics Calculations

The calculation of sample power generation was basically a physics problem and was considered in two parts: (1) the physical model assumed and (2) the calculational method utilized. Since the first of these factors depended upon the physical makeup of the capsule and fuel pin, an audit of the design, fabrication, and assembly of these components was conducted including the following:

a. Chemical analysis of a pellet from the pin II-A batch showed 20.0 ± 0.4 percent Pu content.

b. X-rays of the finished fuel pin were checked to verify the correct length and number of pellets. Insulator pellets were distinguished from fuel pellets by their length.

c. No evidence could be found that any materials substitutions were made in fabrication or assembly. The accidental use of boron steel was very unlikely due to the difficulty encountered in welding this material.

d. Chemical analysis was conducted on the Thermoflex insulation material and no significant amounts of neutron absorbers were found (boron ~100 ppm).

e. A cross-check of the physics model and the as-built capsule drawings revealed a small amount of additional steel not considered in the original calculation of power generation.

Thus, the physical model was revised to account for (e) above, and sample power generation recalculated using a corrected method of normalization to the TREAT core. It was found

that the original normalization was based upon an erroneous reactor size. Renormalization, based upon the actual reactor configuration used in the test increased the absolute flux level to a value which checks very well with the Series I test results. This higher level has been substantiated by data from a plutonium fission chamber placed at the capsule surface. Thus, changes in the physical model and renormalization reduced the computed average power density from $2.33 \times 10^{-4} P_T$ to $1.67 \times 10^{-4} P_T$ $(\frac{\text{Watts}}{\text{cm}^3})$, or a factor of 1.4.

It was concluded that the remainder of the discrepancy was a result of a miscalculation of the flux depression (either in the pin or in the capsule). A P_3 approximation to transport theory was used to obtain the thermal neutron flux depression in the original computations. This approximation is more accurate than diffusion theory in that it more accurately accounts for the fact that the flux is not isotropic under conditions of high absorption in small regions. However, for extremely highly absorbing regions the P_3 approximation may not be accurate enough and higher order transport theory may be required.

In order to verify the fuel pin power profile, an alternate calculational approach was used to obtain the thermal flux depression in the sample. This approach involved the use of a "single collision removal" theory in the fuel, in which the average to surface flux takes the form:

$$\frac{\Phi}{\Phi_s} = \frac{2(1-e^{-\Sigma_a D})}{\Sigma_a D(1 + e^{-\Sigma_a D})}$$

where, Σ_a = macroscopic fuel absorption cross section

and D = fuel diameter

This method resulted in essentially the same flux depression in the sample as obtained from the P_3 calculations. Further, recent irradiations in GETR also indicate that the P_3 flux distribution in the sample is correct.

It appears, therefore, that the majority of the large apparent flux depression is in the capsule. This conclusion is being further investigated using a one dimensional, thermal flux code, THERMOS, to evaluate the effect of Pu239 self-shielding in the sample. A two-dimensional calculation will be required to accurately determine geometry effects in the capsule. Figure 4-1 shows the expected power density as a function of radius in the specimen.

4.2.3 Experimental Results

Based on the above study, heat transfer computer calculations (TIGER V) were rerun using the new power generation relationships, and it was indicated that a ~150 MWsec (0.19 sec initial period) would be necessary to reach melting in the fuel pin (see Figure 4-2). Accordingly, a 155 MWsec transient was run on February 8, 1963, resulting in a capsule equilibrium temperature rise very near the 250 F expected (see Figure 4-3). The capsule reached an equilibrium temperature condition (ΔT = 238 ± 23 F) some 30 seconds after the transient. Adjusting for the apparent capsule heat loss during this period, a total sample energy release of ~56 Btu was calculated for the 155 MWsec transient.

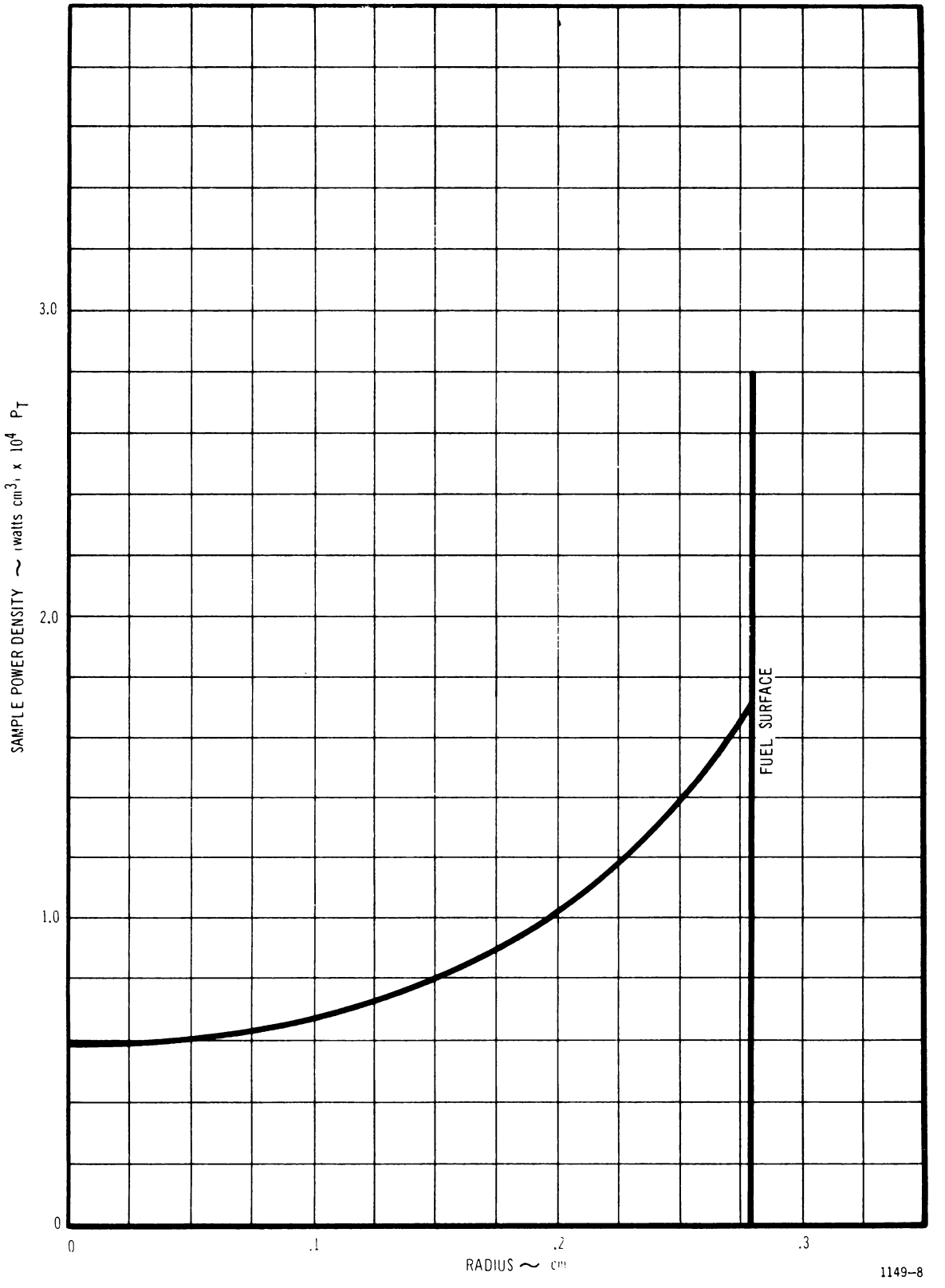

Figure 4-1. Sample Power Density As A Function of Radius

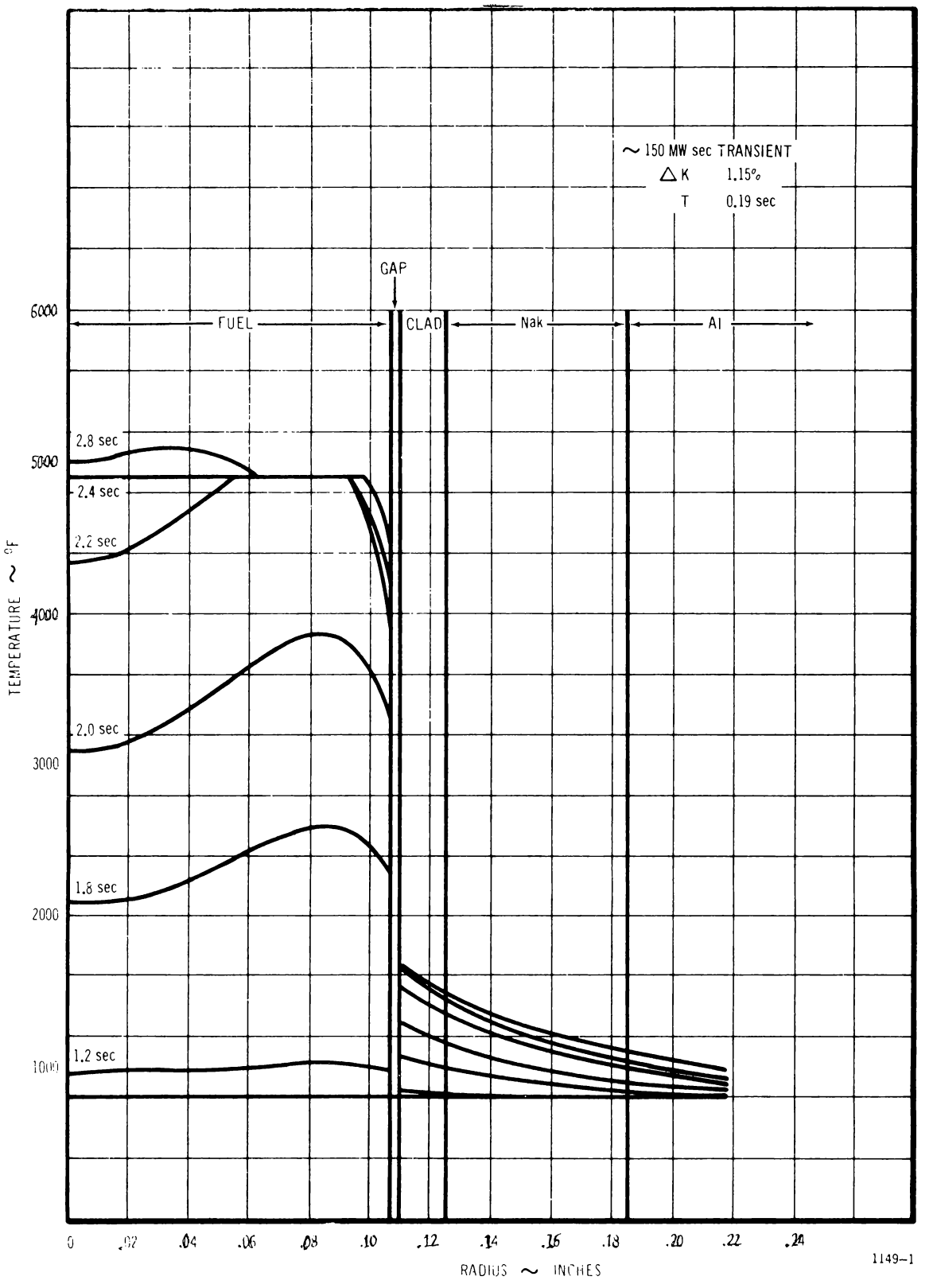

Figure 4-2. Radial Temperature Profiles (Computed)

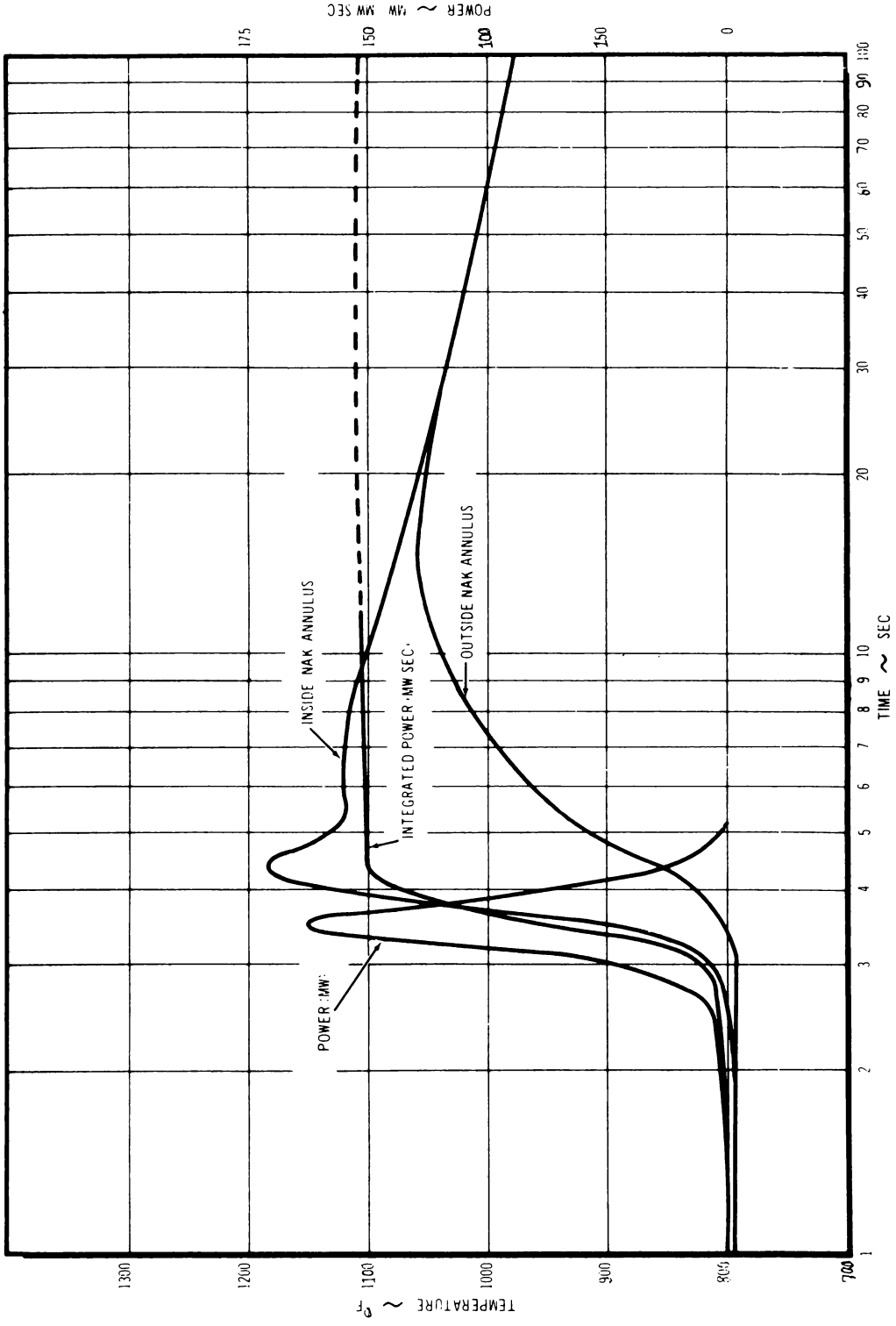

Figure 4-3. TREAT Transient for Sample II-A - 155 MW-Sec

Gamma radiation analysis indicated a total energy release in the fuel of $2.7 \pm 0.3 \times 10^{-2}$ MWD T or ~82 Btu for the two transients. This translated into 23 Btu for the 60 MWsec transient and 59 Btu for the 155 MWsec transient, which agreed within five percent of the values derived above from measured thermocouple data and calculated heat capacity.

Attempts were made to simulate the second transient using the TIGER V computer code and the measured power input data. Relatively good agreement has been obtained between measured and computed NaK temperatures based on the transient power density from measured calorimetric data. This comparison indicated that the revised method of calculation of transient power distribution was essentially correct and should be utilized in future tests. This calculational model results in an indicated peak fuel temperature for the 155 MWsec transient of ~4900 F plus some small portion of the heat of fusion.

4.2.3.1 Post-irradiation Examination

The shipping cask containing the TREAT irradiated II-A assembly was examined and surveyed for gamma activity in the RML decontamination room. Activity readings indicated a maximum of 300 mr hr at the fueled portion of the sample and the portion of the inner capsule covered by the heater was darkened and somewhat rougher than the remainder of the capsule wall. The subassembly was photographed and the disassembly resumed. The NaK fill and vent tubes were exposed and the internal gas pressure released. Both the fill and vent tubes were opened by sectioning with an abrasive wheel and approximately 5 cc of NaK removed through the vent tube, reacted, and analyzed for plutonium.

No plutonium was detected in the sample and it was, therefore, considered safe to continue the disassembly. The remaining NaK was reacted, and the fuel pin removed by cutting off the top spacer and machining off the weld of the pin to the bottom spacer.

The fuel pin was bowed to some extent, and was darkened in the region of the active fuel material. Dimensional measurements performed on the fuel pin indicated a maximum bow of 0.1-inch, and a corresponding decrease in length of 0.003-inch. No change in the OD dimensions was observed, within the accuracy of the measurement technique (+0.5 mil).

The burnup of the Series II-A fuel pin ($2.7 \pm 0.3 \times 10^{-2}$ MWD/T, see above) was determined from a gamma spectrum of the fuel pin obtained at low geometry using the 1.60 Mev photopeak of La-140 in equilibrium with the Ba-140. The spectrum was obtained with a 1-3/4 inch by 2 inch NaI (T1) crystal optically coupled to a Dumont 6292 phototube. After amplification, the pulses were fed into a 400-channel TMC pulse-height analyzer.

In order to determine the geometry for this extended source, the axial distribution of gamma activity was determined as follows. The pin was shielded from the detector, with only a 1/2 inch slit in the shielding existing perpendicular to the long axis of the fuel pin.

An axial scan of the fuel pin was made by moving the pin in 1/2 inch increments in front of this collimating slit and obtaining the spectrum for each increment with the detector placed 2 feet away. The spectra showed that essentially all of the gamma activity was located in a six-inch section of the fuel rod (fuel section) and had a relatively flat distribution of activity over this region.

The detector was moved back to four feet and a gamma ray spectrum obtained of the unshielded fuel rod oriented with the long axis perpendicular to the face of the crystal. At this distance, the counting efficiency for an extended source of 6 inches was found to be about 1 percent. This was determined by arranging six Cs-137 sources having count rates of 5×10^3 dpm in various distributions.

Four peaks were in evidence in the gamma spectrum having energies of 0.50, 0.60, 0.75, and 1.60 Mev with the 0.50 Mev peak the predominant one. After subtraction of the background, the total number of events in the La-140 1.60 Mev photopeak was used for the burnup determination. The 0.75 Mev peak was found to contain activities other than Zr-95, Nb-95 by detailed investigation of the spectrum and, therefore, was not used for the burnup determination. The 0.50 and 0.60 Mev peaks were also complex.

The initial rough-cut section of the fuel revealed an internal appearance much like that of early Series I samples. There was evidence of extensive radial fuel cracking and metallography may reveal some grain growth, but no central void or other indication of molten material was found (see Figure 4-4). No evidence of pellet-to-pellet sintering was observed but the fuel-clad gap is greatly reduced, as evidenced by the apparent immobility of the pellets within the cladding.

4.3 Series III Tests

Pre-irradiation of Series III fuel specimens (0.25 inch diameter, mixed oxide) was delayed pending a decision on test reactor assignment. Based on a technical evaluation to determine the suitability of alternate facilities, it was concluded that the requirements for the pre-irradiation of Series III specimens, in particularly control of $\int k d\theta$, could best be fulfilled in GETR. Accordingly, capsules III-A and III-B were prepared for insertion in the GETR pool positions X9 and X10 during cycle 42. Fabrication of the remaining capsules was initiated with III-C, D, and E scheduled for GETR insertion in cycle 44.

4.4 References

1. Field, J. H., Experimental Studies of Transient Effects in Fast Reactor Fuels, Series I, UO_2 Irradiations, GEAP-4130, November 15, 1962.

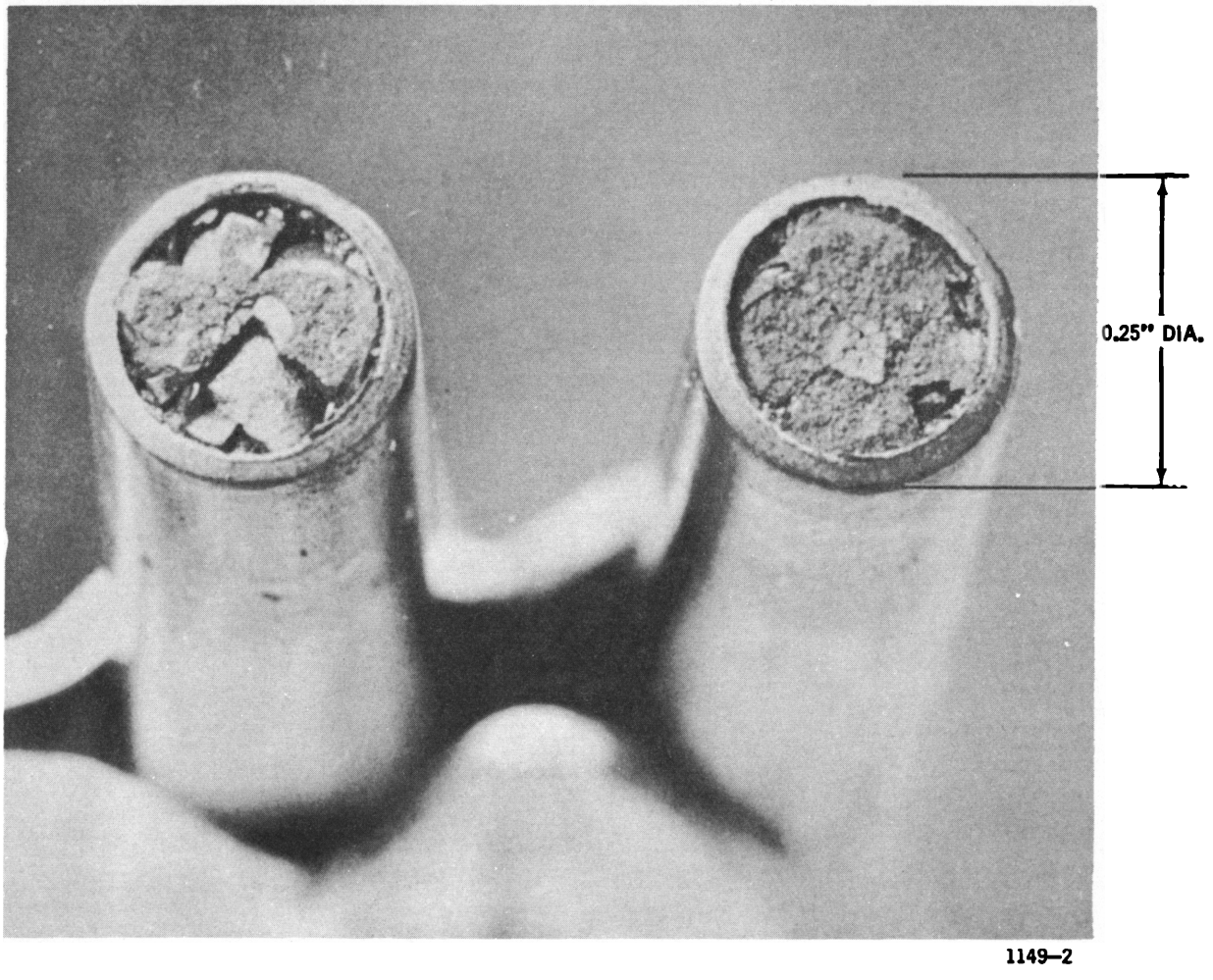

Figure 4-4. Rough Transverse Section II-A

SECTION V

TASK E - FUEL PERFORMANCE EVALUATION

5.1 Central Temperature Measurement of Mixed Oxide

Preliminary capsule design has been completed for a capsule which will carry two fuel pins equipped with gas thermometers for central temperature measurement. One pin will contain mixed oxide (20 percent PuO_2-80 percent UO_2), the other will contain UO_2 only. Shop design is now in progress. Confirmation of gas thermometer behavior will be done by means of tungsten-rhenium thermocouples up to the temperature limits of the thermocouples. Procurement of tungsten and tungsten-rhenium tubing and compensated thermocouples is underway.

Specifications for fabrication of hollow mixed oxide pellets were released for fabrication development. Fabrication of bushings (pellets with axial central holes) by pressing and sintering was successfully tested. Dies for forming various sizes of annular pellets were designed and ordered. The temperature limitations of W-26 percent Re thermocouples in contact with UO_2 - PuO_2 is not known. The high temperature compatibility of mixed oxide with tungsten, tungsten-26 percent rhenium alloy, and with pure rhenium, is being determined by sealing small quantities of mixed oxide in capillary tubes of these materials and heating the tubes electrically to temperatures near or above the melting point of the oxide. Metallographic examination of cross sectioned tubes will determine the extent, if any, of chemical attack by the oxide at the metal surface. Rhenium tubing and rod for end plugs and electrical connection to the tubes are on hand and the other materials are in procurement.

A mockup of a tungsten-clad segment of hollow UO_2 pellets attached to a pressure transducer is being assembled in order to investigate the effect of oxide vapor transport upon operation of a gas thermometer capsule. Furnace design for out-of-pile inter-calibration of the gas thermometer with W-Re thermocouples and with a pyrometer was completed and the parts have been fabricated.

Completion of E1A capsule is now scheduled for July 1963, with irradiation starting in August.

5.2 High-Burnup Irradiations

Preliminary capsule designs were completed for (a) reference FCR operating condition irradiations and (b) accelerated irradiations at high specific power, using 0.150 inch diameter pins. Detailed design and procurement is underway.

The irradiations will differ from Phase I irradiations in that the stoichiometry of the fuel will be controlled at 1.97, 2.00, and 2.04, respectively, and that constant power conditions will be maintained.

Progress on the production of mixed oxide fuel samples of specified O/M ratios is reported in following sections.

5.3 Plutonium Migration

The feasibility of using plutonium-242 as a tracer for measurement of migration and self-diffusion of plutonium has been evaluated. It is concluded that excellent sensitivity in migration measurements can be obtained with plutonium-242 tracer, with only minor corrections for background from plutonium-241 captures, at irradiations up to at least 20,000 MWD/T.

The isotopic composition of two samples previously irradiated in Phase I is given in Table V-1.

TABLE V-1

BUILDUP OF PLUTONIUM ISOTOPES IN CAPSULE IRRADIATIONS

Sample[a]	MWD/T × 10^3[b]	Percent of all Plutonium Atoms Remaining			
		49	40	41	42
C-7	52	87.33	11.31	1.096	0.068
9906	81	85.37	13.37	1.19	0.072

(a) Samples taken from specimens V-1-S and V-2-P (See GEAP-3811, page 36 and GEAP-3833, page 10). Samples taken at mid-radius from 0.150 inch OD fuel body.

(b) MWD/T based on plutonium isotopic analysis and plutonium-239/uranium-238 ratios.

The low concentration of plutonium-242 in these unspiked samples indicates that only a small correction would be required for the plutonium-242 formed on irradiation.

Means for spiking plutonium-242 tracer for migration and self-diffusion measurements in mixed oxide fuel are being evaluated. The most promising approach appears to be evaporation of the spike in the form of PuO_2 or mixed oxide from a tungsten or tantalum filament, condensing on a sintered pellet. Tests are scheduled to determine spatial distributions obtainable on solid and hollow pellets.

5.3.1 Capsule Design

A capsule containing six pins differing in stoichiometry and in peak temperature has been designed. The pin at highest temperature is expected to permit measurement of plutonium-242

diffusion in the solid and liquid phase, and also transport via the vapor phase in a pre-formed central void.

5.3.2 Core Sampling

Sampling capable of fine spatial resolution and avoidance of cross-contamination is required for both plutonium and fission product migration measurements. The use of an ultrasonic core drill was investigated to obtain small core samples for plutonium migration studies. A 0.032 inch OD by 0.006 inch wall hypodermic needle was tested on UO_2 pellets. Penetrations of 10 mils into the UO_2 removed an annular ring of material corresponding to the cross section of the hypodermic needle and left a free-standing core of UO_2 slightly smaller than the ID of the needle. Application of this technique promises a method of obtaining small, massive, uncontaminated samples for plutonium migration and self-diffusion studies. This technique was described to Hanford people who have interests in fission product migration. They have since succeeded in obtaining 0.015 inch × 0.085 inch samples from UO_2 pellets by ultrasonic core drilling.

5.4 Fuel Composition and Properties

5.4.1 Gravimetric Determination of Oxygen/Metal Ratio

Studies of the rate of oxidation in air at 750 C and of the rate of reduction in dry hydrogen-helium mixture at 700 C have been completed for sintered 20 percent PuO_2-80 percent UO_2 mixed oxide samples. These oxidation and reduction rates for powder samples are given in Figure 5-1; for pellets, in Figure 5-2. The following is concluded from the data:

(1) The time required for reduction to stoichiometric O/M ratio at 700 C varies up to six hours depending upon the extent to which the pellet has been oxidized.

(2) The 20 percent PuO_2-80 percent UO_2 solid solution takes up less oxygen than would be expected if the products were U_3O_8 and PuO_2. The maximum to which either pellets or powdered samples could be oxidized at 750 C in air corresponded to an O/M ratio of 2.340 (theoretical is 2.533 for 20 percent PuO_2-80 percent U_3O_8).

(3) No decrepitation of 20 percent PuO_2-80 percent UO_2 sintered pellets occurs upon oxidation-reduction cycling.

(4) The density of pellets decreases by about one percent when the O M ratio is adjusted from 1.987 to 2.000.

(5) In the O M determination, the extent to which the samples are oxidized above stoichiometric is not important. Values for O M of 1.986 ± 0.001 were obtained for four similar pellets, although the oxidation time was varied from 5 to 80 minutes.

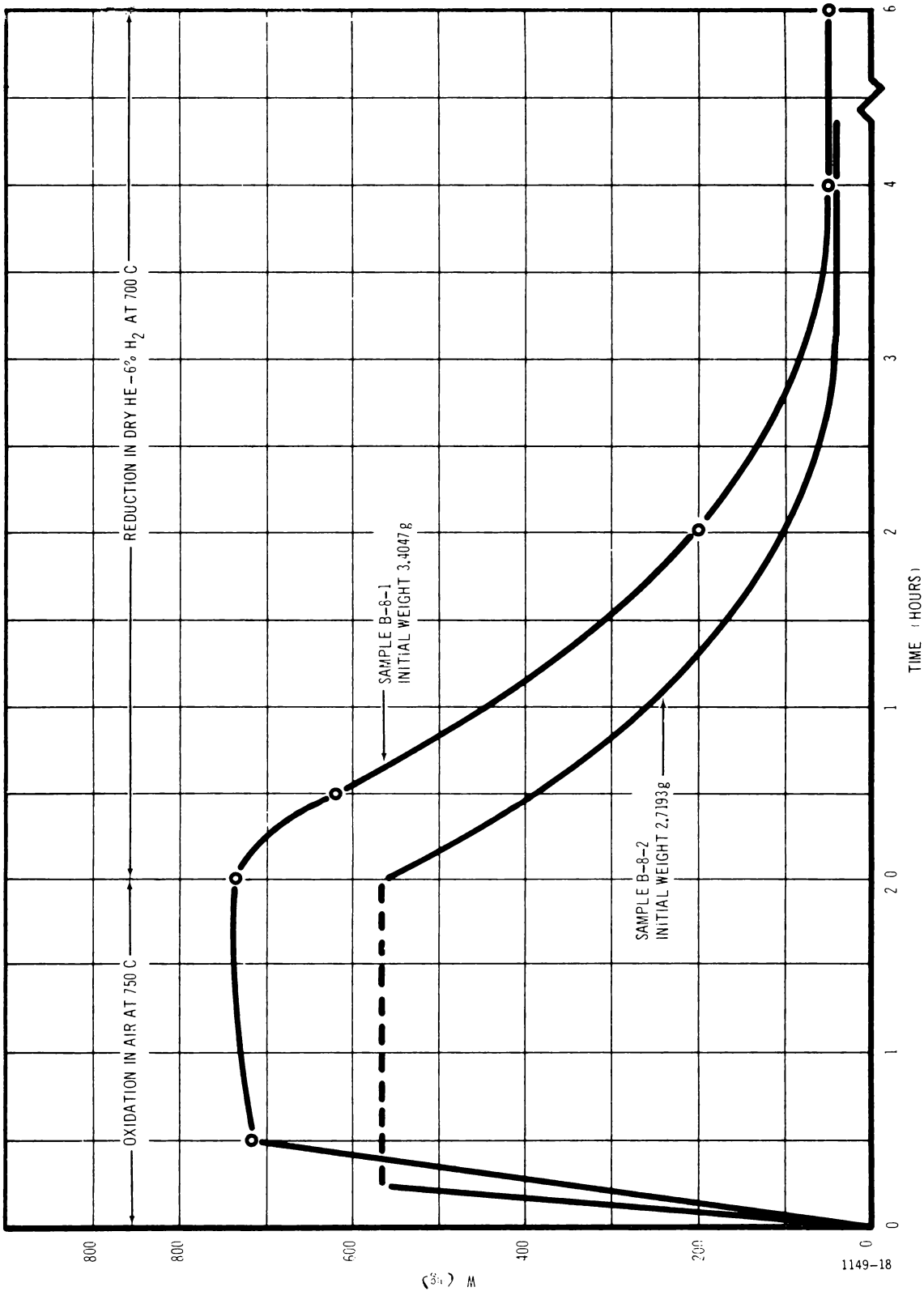

Figure 5-1. Oxidation and Reduction of 20 Percent PuO_2-UO_2 Powder

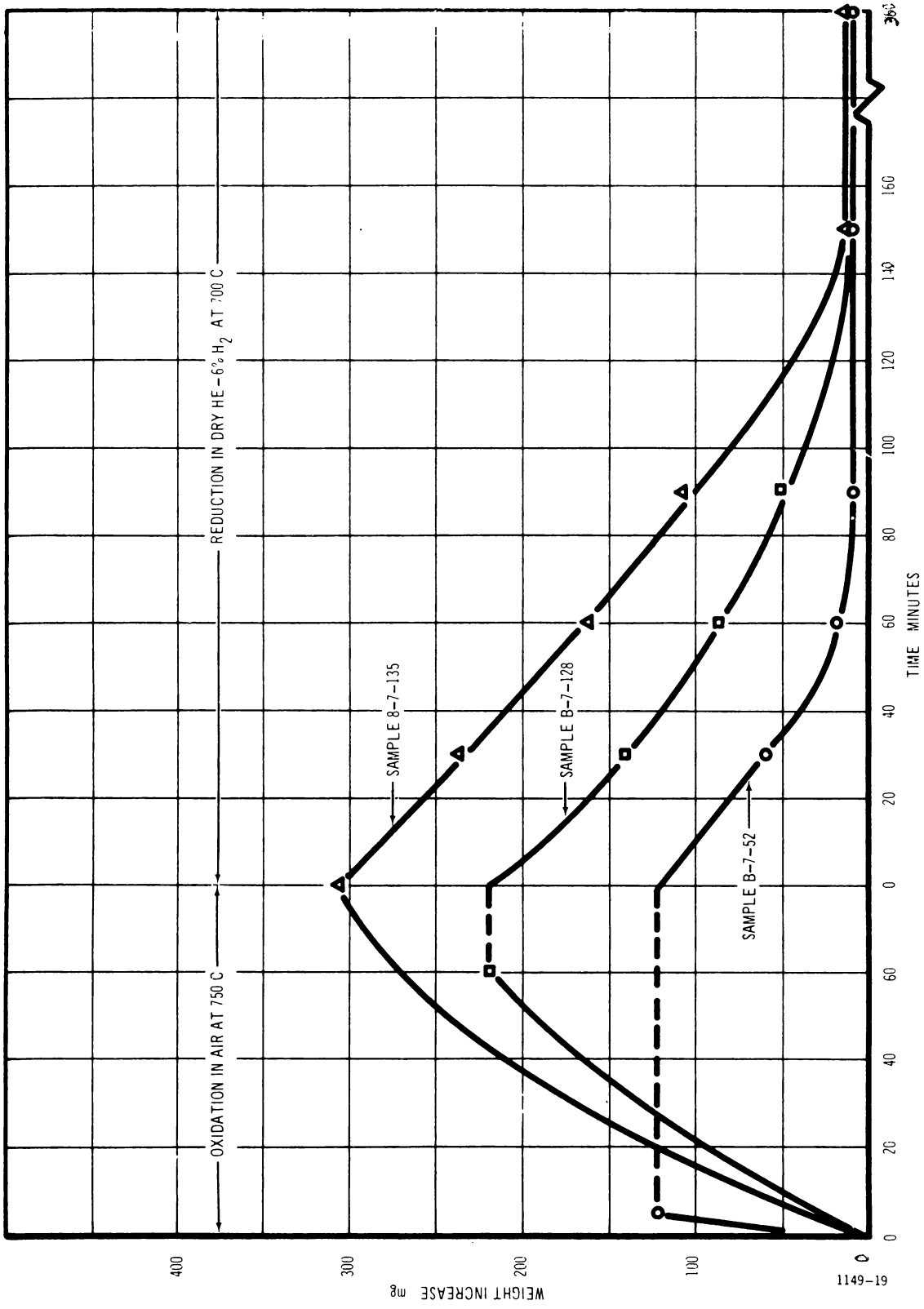

Figure 5-2. Oxidation and Reduction of 20 Percent PuO_2-UO_2 Pellets

Based on the foregoing observations, a gravimetric technique has been developed which provides a reliable measurement of O/M ratio applicable to unirradiated mixed oxide fuel samples. The method, based upon an equilibrium weight at 700 C in dry helium - 6 percent hydrogen gas, was shown to be capable of measurement of O/(Pu + U) ratios in UO_2-20 percent PuO_2 with a standard deviation of ± 0.001.

The analytical procedure adopted is as follows:

(1) Heat the sample in dry argon gas about one hour at 110 C until constant weight W_1 is obtained.

(2) Heat to 750 C in air for ten minutes.

(3) Reduce in dry (magnesium perchlorate drying column) 6 percent H_2-94 percent He at 700 C until a constant weight, W_2 is obtained (~2-1/2 hours).

The value O M is calculated as

$$O\ M = 2.000 - \frac{M}{16}\left(\frac{W_2 - W_1}{W_2}\right)$$

where M is the average molecular weight of the stoichiometric oxide mixture.

Values for O M as determined in sintered pellet samples are given in Table V-2.

Analyses of the mixed oxide ceramic powders used for these pellets indicates that O/M ratios are 2.110 to 2.182 prior to pressing and sintering.

The glove box and equipment used for gravimetric determination of O/M ratio is shown in Figure 5-3.

5.4.2 Optical and Infrared Spectrometric Determination of Oxygen Stoichiometry

Optical techniques have been explored for the analysis of pellets for oxygen stoichiometry. Reflectance spectra versus a magnesium carbonate standard were run for samples of UO_2, UO_{2+x}, U_3O_8 and UO_3 in the wave length range 240 to 750 millimicrons. Although differences in the percent reflectance were observed, as anticipated, well-defined peaks, which could serve as a basis for quantitative measurement of oxygen-to-metal ratio, were not found.

Oxide samples were also scanned for fluorescence in the 400 to 800 millimicron region when illuminated with 300 to 400 millimocron light. No fluorescence was observed.

TABLE V-2

OXYGEN TO METAL RATIOS IN FCR FUEL SAMPLES

Batch Number	Pellet Numbers	Nominal Composition	Sintering Atmosphere	Average O/M Ratio
B-2	94, 89	UO_2-20% PuO_2	He-6% H_2 as received	1.982 ± 0.009
B-3	4, 96	UO_2-20.6% PuO_2	He-6% H_2 as received	1.980 ± 0.012
B-4	116, 117	UO_2-28.1% PuO_2	He-6% H_2 as received	1.979 ± 0.006
B-5	51, 76	UO_2-19.9% PuO_2	He-6% H_2 as received	1.991 ± 0.005
B-6	45, 79	UO_2-22.5% PuO_2	He-6% H_2 as received	1.972 ± 0.019
B-7	84, 157-162, incl.	UO_2-19.7% PuO_2	He-6% H_2 as received	1.978 ± 0.010
B-7	52, 94, 128, 135	UO_2-19.7% PuO_2	He-6% H_2 as received	1.986 ± 0.001
B-8	(six pellets not identified)	UO_2-19.9% PuO_2	He-6% H_2 as received	1.972 ± 0.001
B-8	137 - 140, Incl.	UO_2-20% PuO_2	He-6% H_2 with H_2O addition	1.998 ± 0.001
B-9	134, 137	UO_2-20% PuO_2	He-6% H_2 with H_2O addition	2.000 ± 0.001
U-5	7	UO_2	He-6% H_2 as received	2.007
P-2	3	PuO_2	He-6% H_2 as received	1.850

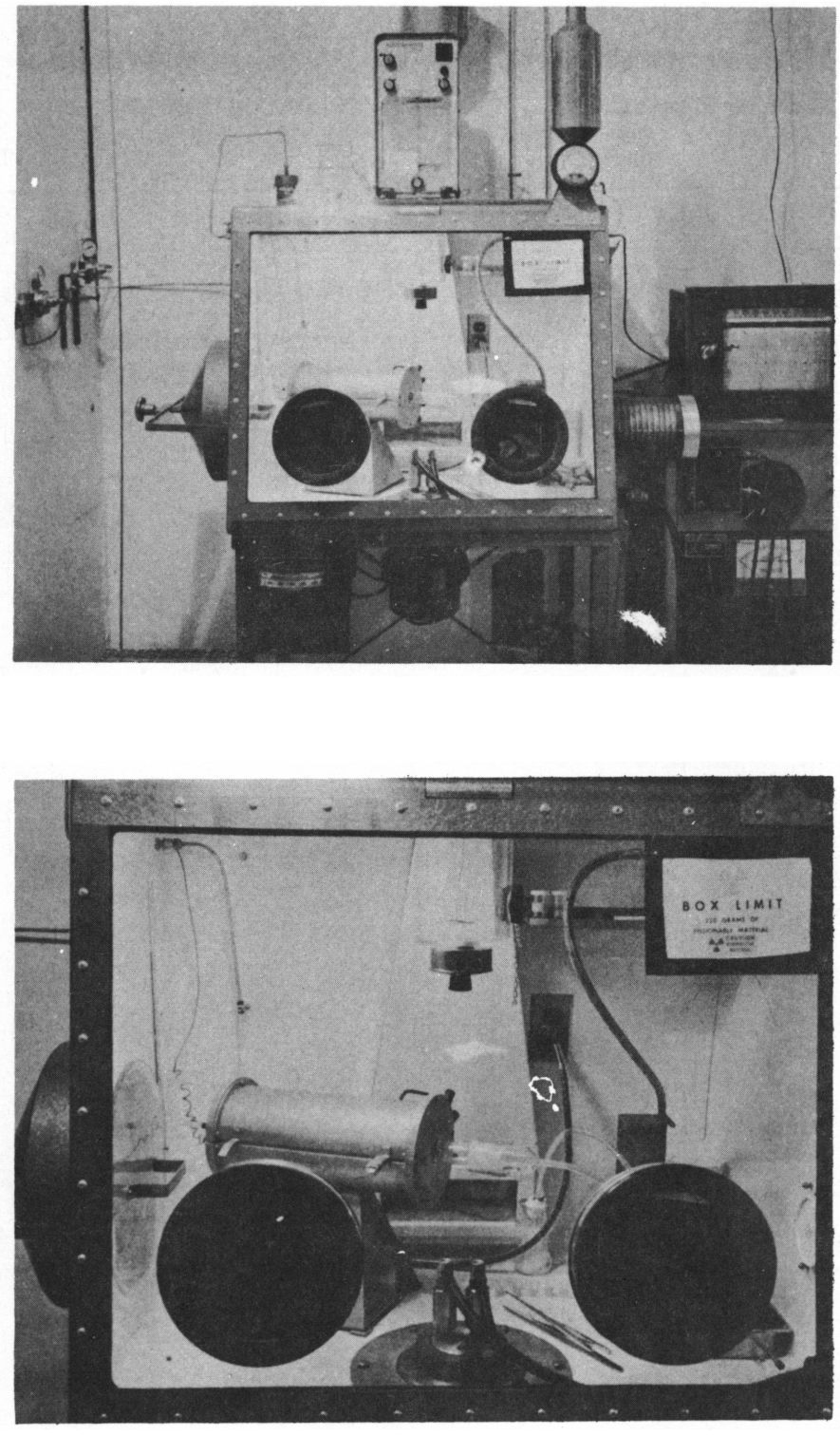

1149–20

Figure 5-3. Facility for Gravimetric Determination of O/M in Mixed Oxide

Infrared absorption spectra were obtained in the region 2 to 15 microns using the KBr pellet technique. Peaks were observed at 10.7 and 13.6 microns for both U_3O_8 and UO_3, and at 11.6 for UO_3. These peaks were not found in the UO_{2+x} spectrum. The method does not appear promising for analytical use in the oxygen-metal region of interest.

5.4.3 Melting Point and X-Ray Study of Mixed Oxides

The apparatus for determination of melting points of mixed oxide fuel in an atmosphere of oxygen at high pressures was assembled and tested. Calibration of the two-color pyrometer using samples of known melting point is underway. Difficulties have been found in observing the thermal arrests on melting of UO_2. Samples of mixed oxide fuel with varying PuO_2 content will be used for a study of melting point versus composition. X-ray equipment for diffraction and fluorescence measurements on mixed oxides has been installed and aligned, and will be used to characterize the melting point samples.

5.4.4 Properties of Mixed Oxides Prepared via Coprecipitation

Mixed oxide batches with the plutonium content varied from five to 90 percent were prepared on a 10 gram scale to furnish specimens for x-ray, melting point, and other property studies as function of composition. In the batch precipitations, there was observed a marked improvement in rates of settling, filtration, and drying when the Pu/U ratio was near unity. Similarly, an increase in the tap density of the mixed oxide powders was observed near the middle of the composition range as shown in Table V-3.

TABLE V-3

TAP DENSITY OF MIXED POWDERS PREPARED VIA COPRECIPITATION

Percent PuO_2	Tap Density (g/cc)
0 (UO_2)	2.1 - 2.7
5	2.1
10	2.1
15	2.8
20	(3.1 - 3.6)*
40	4.6
50	5.4
60	6.0
70	5.8
80	5.1
90	5.3
100	3.4**

* Data from full-scale batches.

** NUMEC data, NUMEC P-103.

Dissolution of unsintered samples of the mixed oxide powders in nitric acid revealed that the compositions of greater than 40 mol percent PuO_2 contained some of a second phase (presumably PuO_2) which was not solid solution mixed oxide, i.e., a nitric acid-HF mixture was necessary for complete dissolution.

The sintered composition containing five percent PuO_2 was found to breakdown completely to powder upon heating to 750 C in air. The 10 percent PuO_2-90 percent UO_2 pellet broke up to a lesser extent upon heating in air, but compositions greater than 15 percent PuO_2 retained structural integrity.

5.4.5 Fissia in Mixed Oxide Fuel

The influence of macroscopic fission products and their oxides (fissia) on fuel properties is expected to be important at high burnup. In addition to irradiated specimens, it may be desirable to prepare synthetic mixtures for preliminary exploration of properties such as effective stoichiometry, conductivity, and diffusion.

The following table (V-4) represents the approximate composition calculated for fuel irradiated for 3.0 years to a peak burnup of 118,000 MWD/T (13.8 percent) at zero cooling time. Because of the long irradiation time, only small differences in chemical composition result from the first few months of cooling, or from longer irradiations at slightly lower specific powers. No correction has been made for neutron captures by fission products. The fission product spectrum is for fast fission of plutonium-239[1], neglecting the differences in yields due to the fraction of fissions from uranium-238 and the higher plutonium isotopes.

5.5 Experimental Fuel Fabrication

5.5.1 Powder Preparation

The use of acetone for drying the ADU-$Pu(OH)_4$ coprecipitate was abandoned for safety reasons and without deleterious effect on the process.

The time for ball-milling of the mixed oxide ceramic powder was reduced from 8 hours to 2 hours. This is expected to result in a lower content of alumina and silica impurities in the mixed oxide fuel.

The process developed for preparing high density granular mixed oxide (direct sintering of compacts of ADU-$Pu(OH)_4$ coprecipitate) previously demonstrated on a small-scale, will be tested on the full batch scale when necessary equipment modifications have been completed. The vibratory compaction development has been deferred pending installation of the new pin loading box.

---

(1) L. Burris and I. Dillon, ANL-5742, June 1957.

TABLE V-4
COMPOSITION OF FISSIA AT 118,000 MWD/T

Element	Weight Percent
U	69.98
Pu	16.20[2]
Kr	0.04
Rb	0.05
Sr	0.20
Y	0.11
Zr	1.06
Nb	0.03
Mo	1.12
Tc	0.33
Ru	1.43
Rh	0.32
Pd	0.96
Ag	0.11
Cd	0.07
In	0.01
Sn	0.02
Sb	0.02
Te	0.35
I	0.19
Xe	1.82
Cs	1.36
Ba	0.48
La	0.42
Ce	0.97
Pr	0.36
Nd	1.34
Pm	0.17
Sm	0.42
Eu	0.05
Gd	0.01
Other	0.01
Total	100.00

(2) Fourth Quarterly Report FCR Program, July-September, 1962, GEAP-4080; initial plutonium enrichment of 18.4 percent; equilibrium cycle with recycled plutonium; core breeding ratio of 0.82; 71.3 percent of total fission in plutonium-239.

5.5.2 Fabrication of Mixed Oxide with Controlled Stoichiometry

The fabrication of batches of mixed oxide fuel pellets to specified oxygen/metal stoichiometry is undergoing study. The addition of water vapor directly to the sintering atmosphere, by bubbling 6 percent H_2-94 percent He gas through water, has been shown to result in stoichiometric (O/M = 2.000 ± 0.001) mixed oxide fuel at ~1450 C. This procedure, however, results in low (≈20 percent) yields of pellets of specification density, ≧ 93.5 percent T.D. The use of a dry sintering atmosphere obtained by passing the 6 percent H_2-94 percent He gas through a column packed with magnesium perchlorate, yields pellets whose O/M ratio is about 1.97. Yields of sub-stoichiometric pellets in excess of 90 percent are obtained whose density is greater than 93.5 percent of theoretical density. A two-step process is being tested, using dry gas for densification and wet gas re-oxidation, or air re-oxidation followed by 700 C dry gas reduction.

5.5.3 Pellet Sintering

The temperature profile of the molybdenum boat during sintering was investigated. An optical pyrometer target at the mid-point of the boat indicated a temperature approximately 40 C higher than at either end of the boat in the range 1500 to 1600 C. It has been frequently observed that pellets located in the front or rear of the boat are less dense than those in the middle. These observations bear out other evidence that the optimum temperature range for sintering is quite narrow.

Pellets were pressed in 0.187 and 0.190 inch diameter dies and sintered to determine approximate process parameters for fabrication of 0.150 inch diameter pellets. Initial results indicate that there should be no major problem in fabricating 0.150 inch pellets and that shrinkage during firing and fired density are comparable to previous data for 0.220 inch diameter pellets.

The effect of firing at approximately 1600 C for two to four hours was investigated with powder batch designated B-8. Very low densities (85 - 88 percent theoretical) were obtained at this temperature, perhaps partially attributable to the condition of the powder in the green state:

	Batch B-7	Batch B-8
Hydraulic Pressure (psig)	135	135
Average Green Density (percent theor)	46-47	43-44
Average Fired Density (percent theor)	92-95	85-88

The B-8 powder had been stored for approximately two months, between powder preparation and pressing, in a glass jar with a screw-on top (no gasket). It was expected that the powder had become highly super-stoichiometric; the oxygen-to-metal ratio was measured to be 2.180. The powder was partly re-reduced to an O M ratio of 2.110. Fired density of the re-reduced powder was 89-93 percent of theoretical as compared to 85-88 percent for the original powder.

A subsequent batch, B-9, was not allowed to age. An initial firing resulted in an average fired density of 97.1 percent of theoretical. The O/M ratio of this powder was found to be 2.182. This result contradicted the view that highly super-stoichiometric powder reduced the final fired density. The physical characteristics of the powder in the green state will be further investigated.

The number of pellets fired at one time was increased threefold (12-35) to determine if larger numbers of pellets could be fired at one time without detrimental density variation. The average deviation in fired density of the larger group was essentially equivalent to previous smaller firings. Also, an investigation was made on the importance of gas coverage over the pellets as they are being fired. Several pellets were shielded from the gas, and several pellets were placed directly in the gas flow. No significant difference in density was obtained; consequently, there are no indications of major problems due to gas distribution in firing larger batches of pellets.

Three experimental sintering runs were made in the small tungsten resistance furnace in attempts to optimize sintering conditions for this equipment. One run was made with water addition to the gas. Specification densities have not yet been achieved from pellets sintered in this furnace, although the same observed temperature region as used in the large molybdenum - wound furnace has been employed.

5.5.4 Plutonium Laboratory Facilities

Procurement was initiated for three new facilities (pin loading glove box, pin decontamination fume hood, and pin welding glove box). These new facilities will provide the following operational improvements: (1) increase the maximum fuel pin length which can be handled from 18 inches to 60 inches; (2) decrease time required for decontamination of fuel pins and equipment; (3) decrease time required and increase capacity for pin loading and welding; and (4) increase pellet fabrication capacity by approximately 25 percent by permitting use of present loading and welding box for inspection and classification of sintered pellets and powder.

SECTION VI

TASK F - FAST FLUX IRRADIATION OF FUEL

6.1 Irradiation in EBR-II

To provide performance data on FCR type fuel specimens under representative fast flux exposure conditions, irradiation in EBR-II of an assembly containing 19 mixed oxide fuel specimens has been proposed. Effort on this irradiation, last reported in GEAP-3981, FCR Quarterly Report for April-June, 1962, has been reactivated with a scheduled delivery to EBR-II in November, 1963. The original test description has been updated and progress has been made in the design and fabrication of the test unit.

The original test description was amended January 9, 1963, to comply with requirements set by EBR-II personnel. A request for reconfirmation of the EBR-II reactor loading date was made January 10, 1963, and the amended test was discussed with EBR-II personnel on March 28 and 29, 1963. The test, as now constituted, consists of a welded assembly containing 19 capsules of FCR type fuel. All fuel specimens will be of mixed oxide fuel with a blanket and fission gas reservoir section contained within the fuel clad. This clad will be leak tested and the specimen will then be encapsulated in another container which will also be leak tested. It is planned to load the test assembly into a blanket position first, inspect the assembly after one or two month's exposure, and then transfer the test to an EBR-II core position. This inspection requires the use of the air cell of the EBR-II fuel cycle facility to cut the test assembly apart, select a capsule for destructive examination and reassemble the test unit using new hex tube hardware, the exposed capsules and a replacement capsule. In addition to the non-destructive capsule inspection at EBR-II, the capsule will be destructively examined for possible fission gas leakage to the capsule and fuel specimen distortion. Although little change from this low exposure in the blanket is expected, this degree of examination is planned to assure integrity of the test before transferring it to the EBR-II core. The pre-irradiation testing of the fabricated capsules will be as originally planned, with the addition of a test to measure the sodium bond between the specimen and the capsule wall.

6.1.1 Fuel Specimens

Detailed design and fabrication of the fuel specimens has been initiated, with fuel pellets and clad parts for the first two fuel specimens now on hand. Blanket pellets will be added and the first specimen is expected to be finished by April 19, 1963. The fuel specimen is shown in Figure 6-1, Dwg. 798D146: the G1 design is for clad parts that can be handled after the planned modification to the Plutonium Fuel Fabrication Facility, and the G2 design is for the clad parts

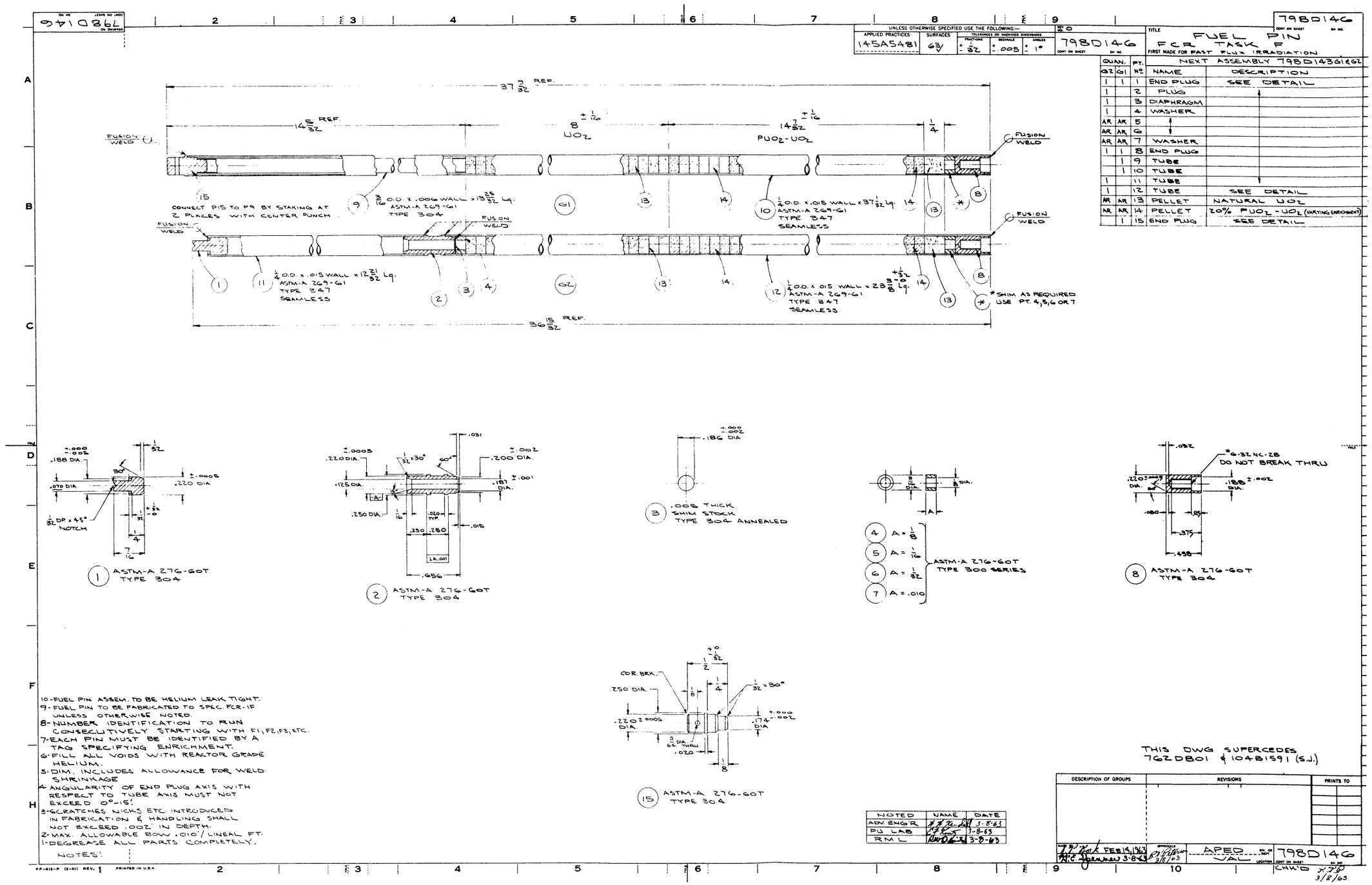

Figure 6-1. Fuel Pin for EBR II Irradiation

that will be used before this modification. Design parameters to be investigated as variables in the 19 pins include the clad-to-fuel gap, O/M ratio in the fuel pellets, axial expansion, core fuel and blanket power, and the clad material. The primary choice for clad material is type 347 stainless steel; other candidate materials are being evaluated for inclusion in this experiment.

6.1.2 Capsules

The detailed design of the capsule is shown in Figure 6-2, Dwg. 798D143, with the fuel specimen and sodium level as indicated. The exterior configuration is still subject to change, depending on the unresolved details of the hex tube assembly design. The internals and filling connections are sufficiently established to permit the design and procurement of the sodium filling equipment. The emphasis on high quality sodium of low oxide content has been increased since it is possible that the irradiation time in EBR-II may be extended over a much longer period than originally expected.

6.1.3 Hex Tube Assembly

Detailed design of the hex tube assembly has been initiated, based on discussions with EBR-II personnel March 28 and 29. The concept for disassembly and reassembly has been changed from the original proposal. Further concept work is being done to select an acceptable capsule spacing method.

6.2 Evaluation of Alternate Facilities

One of the alternate possibilities for a fast flux irradiation would have been use of the fast liquid metal loop which had been planned for the ATR. The loop objectives were re-evaluated at a meeting January 3 at the Chicago Operations Office, at which time it was apparent that the loop was an expensive and belated way of obtaining a fast flux irradiation. An evaluation of alternate facilities for such irradiations was presented by APDA at a meeting February 25 at the same place. From this study it was apparent that EBR-II and the Fermi reactor are the only near-future facilities capable of delivering a satisfactory fast neutron flux. Thus, for Task F purposes, it is planned to direct the major effort toward the EBR-II irradiation described above.

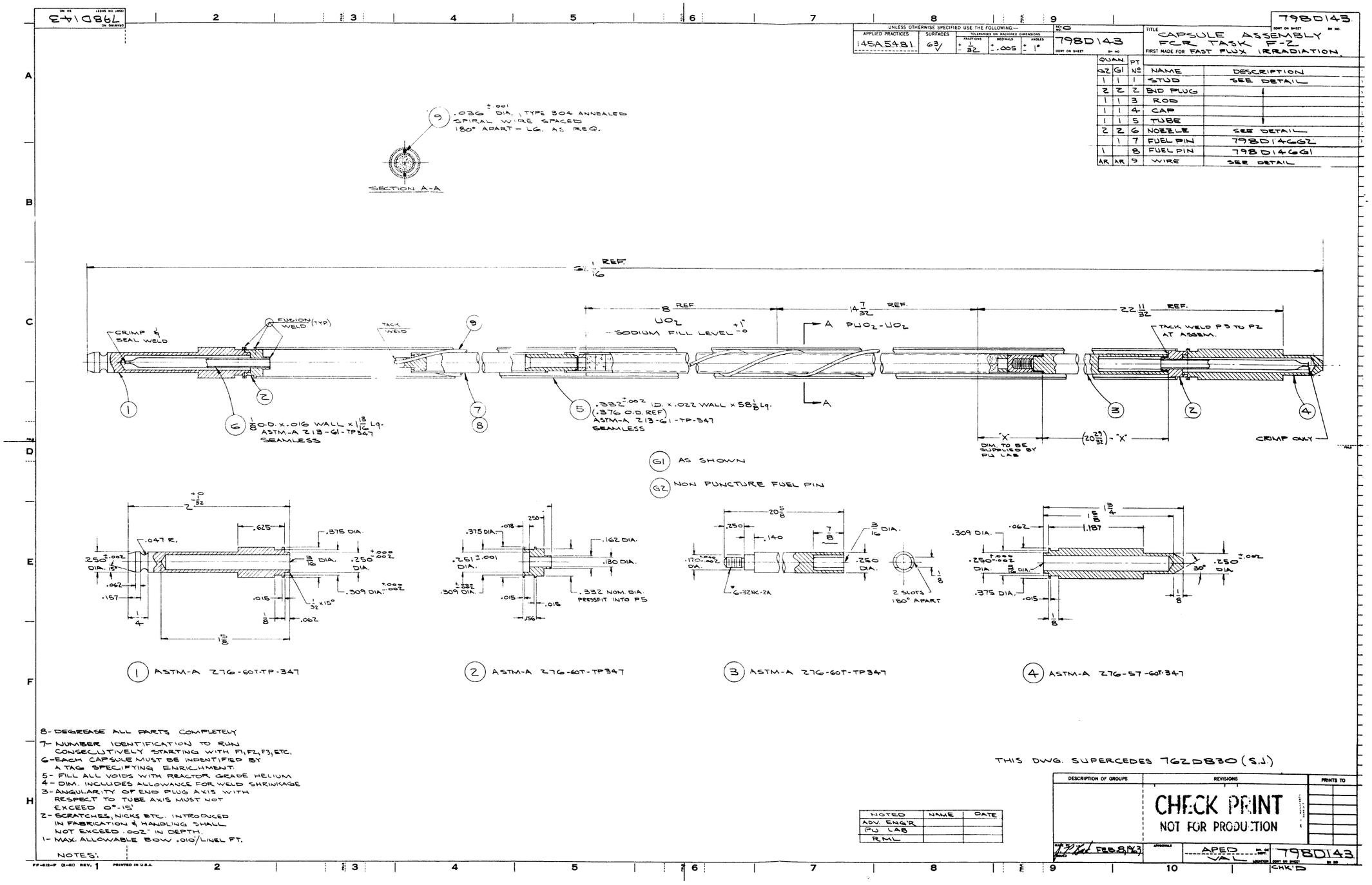

Figure 6-2. Capsule for EBR II Irradiation

SECTION VII

TASK G - REACTOR DYNAMICS AND DESIGN

7.1 Calculations on 1000 MWe FCR

7.1.1 Extreme Pancake Model

Results of the calculations on an extreme pancake model with a 15-inch core height are given in Table VII-1. The values given in the table were computed for a system that is in the hot operating condition and on an equilibrium cycle in a recycle fuel economy. The following assumptions were made to obtain the average equilibrium core and blanket fuel isotopic concentrations used in calculating the parameters in Table VII-1:

a. Maximum fuel exposure at discharge is $100,000 \frac{\text{MWD}}{\text{Ton (U+Pu)}}$.

b. The refueling interval is about 6 months.

c. One-fifth of the fuel is replaced at each refueling.

d. The make-up fuel is obtained from the blankets of an operating FCR.

e. The initial axial blanket fuel is depleted uranium (0.4% enriched in U-235).

f. The core uranium is fully depleted.

The calculated reactivity for the system represented in Table VII-1 is 1.014. The system included an axial 6-inch reflector of 48 percent steel and a radial 6-inch reflector of 80 percent steel. There were no radial blankets used in this model.

The computed reactivity increment when sodium is lost from this pancake core is about 30 percent less than for a similar occurrence in the earlier 500 MW(e) reference design, which has a 3.3 foot core height and a 6.6 foot core diameter.[1] However, the Doppler coefficient was reduced to an unacceptably low value. Consequently, less extreme "pancaking", in conjunction with other modifications such as composition and core blanket configurations, is being evaluated.

7.1.2 Composition Modifications to Improve Safety

Calculations of possible modifications that will minimize the reactivity increment with sodium loss while maintaining a large Doppler coefficient are being made using a simplified model in which there is no net leakage of neutrons from the reactor. Earlier results have shown that the addition of a small amount of BeO will appreciably increase the Doppler coefficient.[1] However, the manner in which the BeO is added, (i.e. homogeneously or in the form

TABLE VII-1

PHYSICS PARAMETERS FOR A PANCAKE MODEL

Core	
Height (feet)	1.25
Diameter (feet)	14.50
Volume (cubic feet)	206
v/o PuO_2-UO_2 (at 9.6 g cm^3 density)	32
v/o Sodium (at 0.83 g/cm^3 density)	52
v/o Stainless steel (Type 304 at 7.8 g/cm^3 density)	16
Top and Bottom Axial Blankets	
Height each (feet)	1.50
Diameter (feet)	14.50
Volume (each) (cubic feet)	247
Same material volume fractions as in the core	
Core Fuel Isotopic Composition (a o)	
Pu-239	14.5
Pu-240	7.1
Pu-241	1.2
Pu-242	0.5
U-238	70.9
F. P. Pairs	5.8
Breeding Ratios for Pu(239+241)	
Core	0.51
Axial blankets	0.82
Total	1.33
Conversion Ratio for Pu(239+241)	
Core	0.60
Doppler Coefficient, (Δk/°C)	
Isothermal at 900 C	-2.0×10^{-6}
Reactivity Change for Total Loss of Sodium, (Δk)	
Axial Calculation	
Core loss only	+0.010

TABLE VII-1 (Continued)
PHYSICS PARAMETERS FOR A PANCAKE MODEL

Operating Reactivity for Burnup	
Δk per 6 months at 800 Kw Kg (Pu-239+ Pu-241) and at 0.8 load factor	-0.016
Neutron Energy Spectrum Indices*	
Fraction of fissions by neutrons below 9 Kev	0.133
Mean neutron energy of power spectrum (Kev)	202
Power Distributions	
Fraction of power in-core	0.8
Fraction of power in axial blankets	0.2
Core radial peak average power	2.25
Core axial peak average power	1.08
Core power density (Kw Liter core)	~340
Core specific power (Kw Kg [Pu-239+ Pu-241])	~800

* Evaluated in the core region of average importance $\emptyset\emptyset^+$, where $\emptyset$ is the neutron flux and $\emptyset^+$ is the adjoint flux.

of hetrogeneous buffers), appears to have a significant effect on the reactivity increment when sodium is lost. Various methods of adding BeO to the system are being evaluated relative to their effect on the sodium loss reactivity increment.

7.2 Reactor Dynamics and Safety

7.2.1 FORE Calculations

Calculations have been performed using the FORE computer code to assess quantitatively the significance of the Doppler coefficient in providing time for the control system to scram the reactor. Some results are shown in Figures 7-1 through 7-5, (for a typical set of FCR parameters taken from the 500 MWe core design) where the ordinate is the time from the beginning of the accidental reactivity insertion to the point at which a peak fuel temperature of 6500 F is reached. This is estimated to be the temperature where significant fuel element deformation occurs.[2,3] The abscissa represents the quantity

$$A_{DOP} \left(\frac{dk}{dT}\right)_{DOP} \times T_{ABS}$$

where $\frac{dk}{dT}$ is the isothermal Doppler coefficient and T_{ABS} is the absolute average core fuel temperature weighted according to the square of the local power density. This quantity is

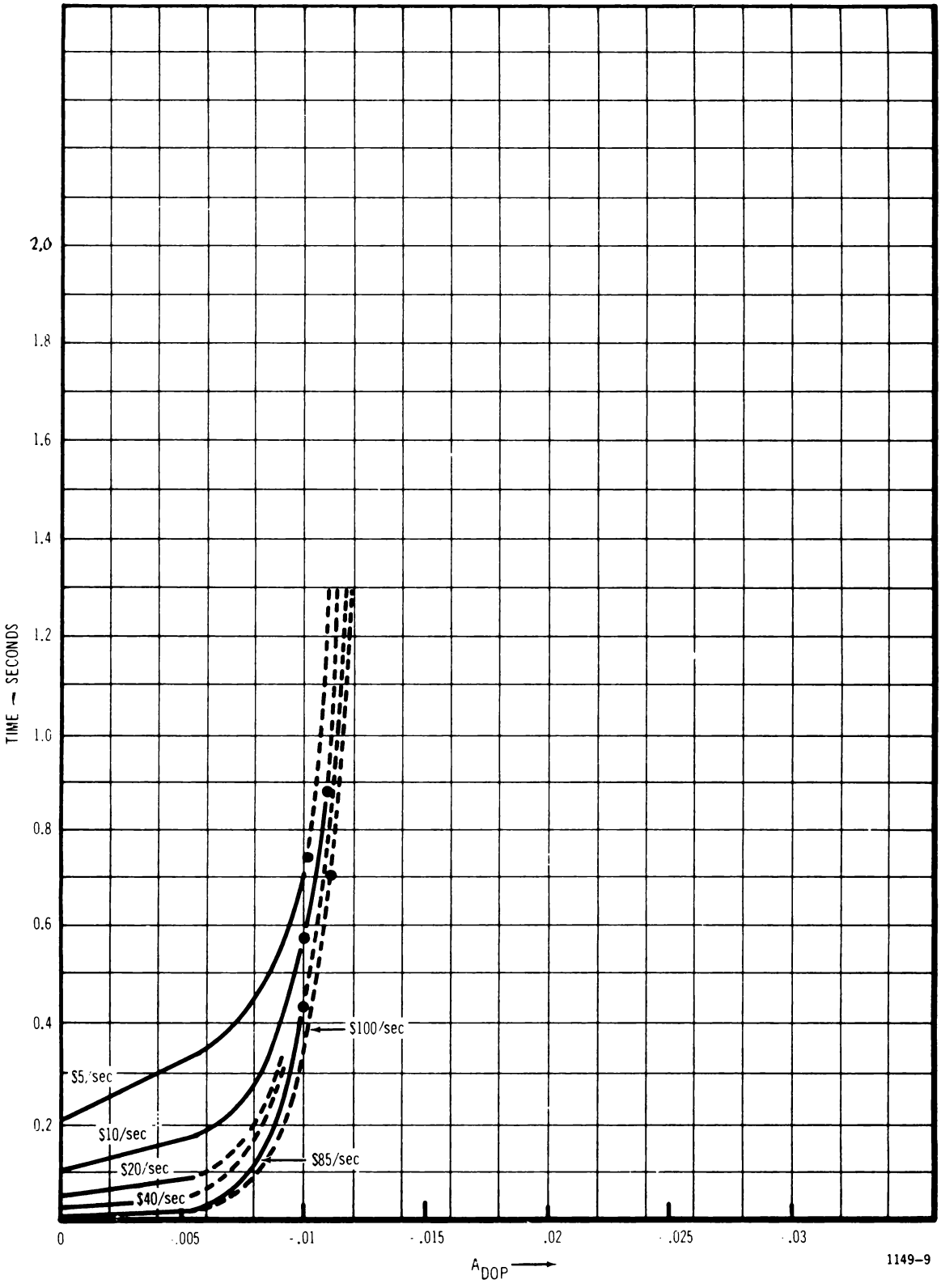

Figure 7-1. Total Reactivity Insertion $1.70

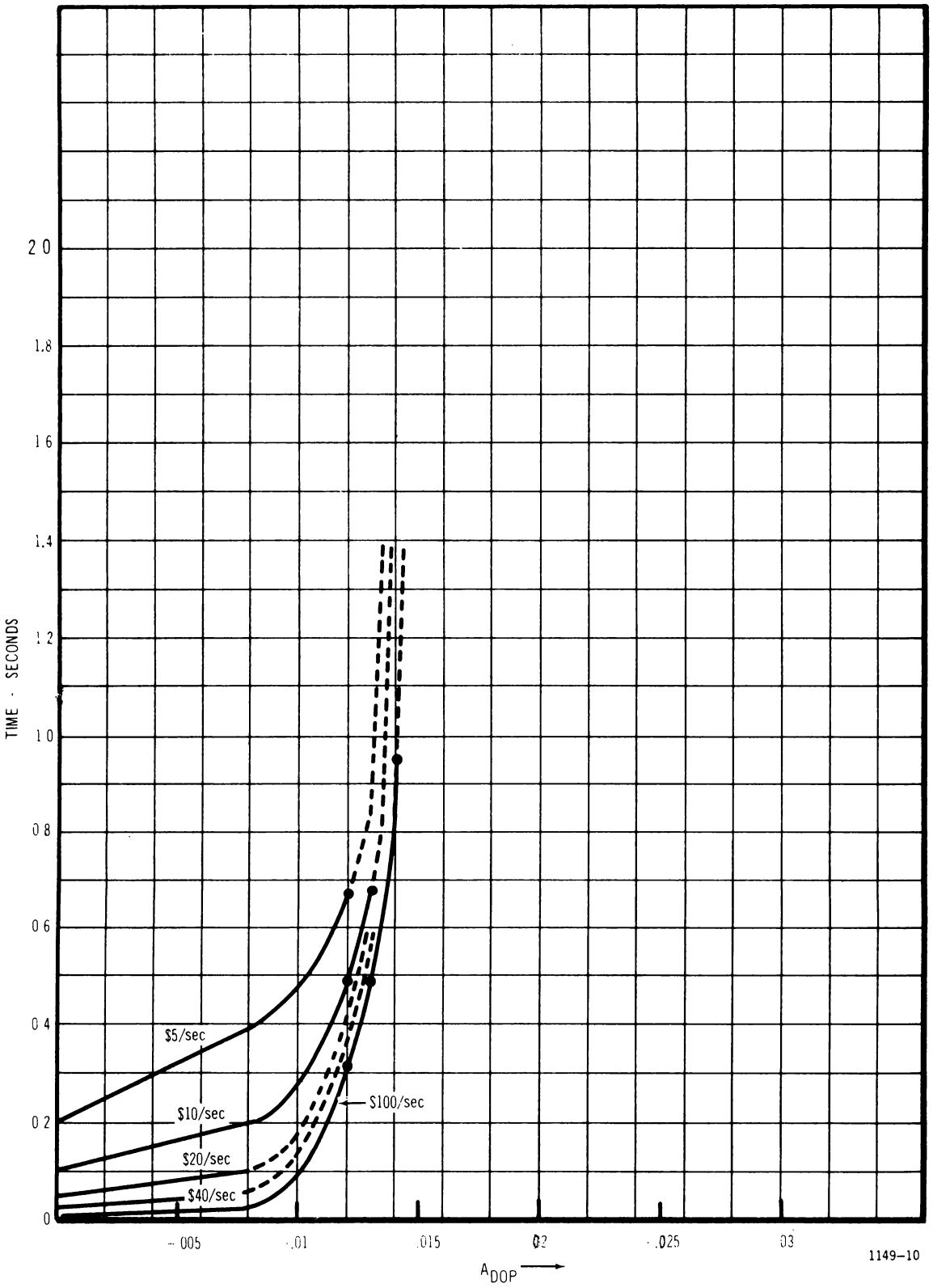

Figure 7-2. Total Reactivity Insertion $2.00

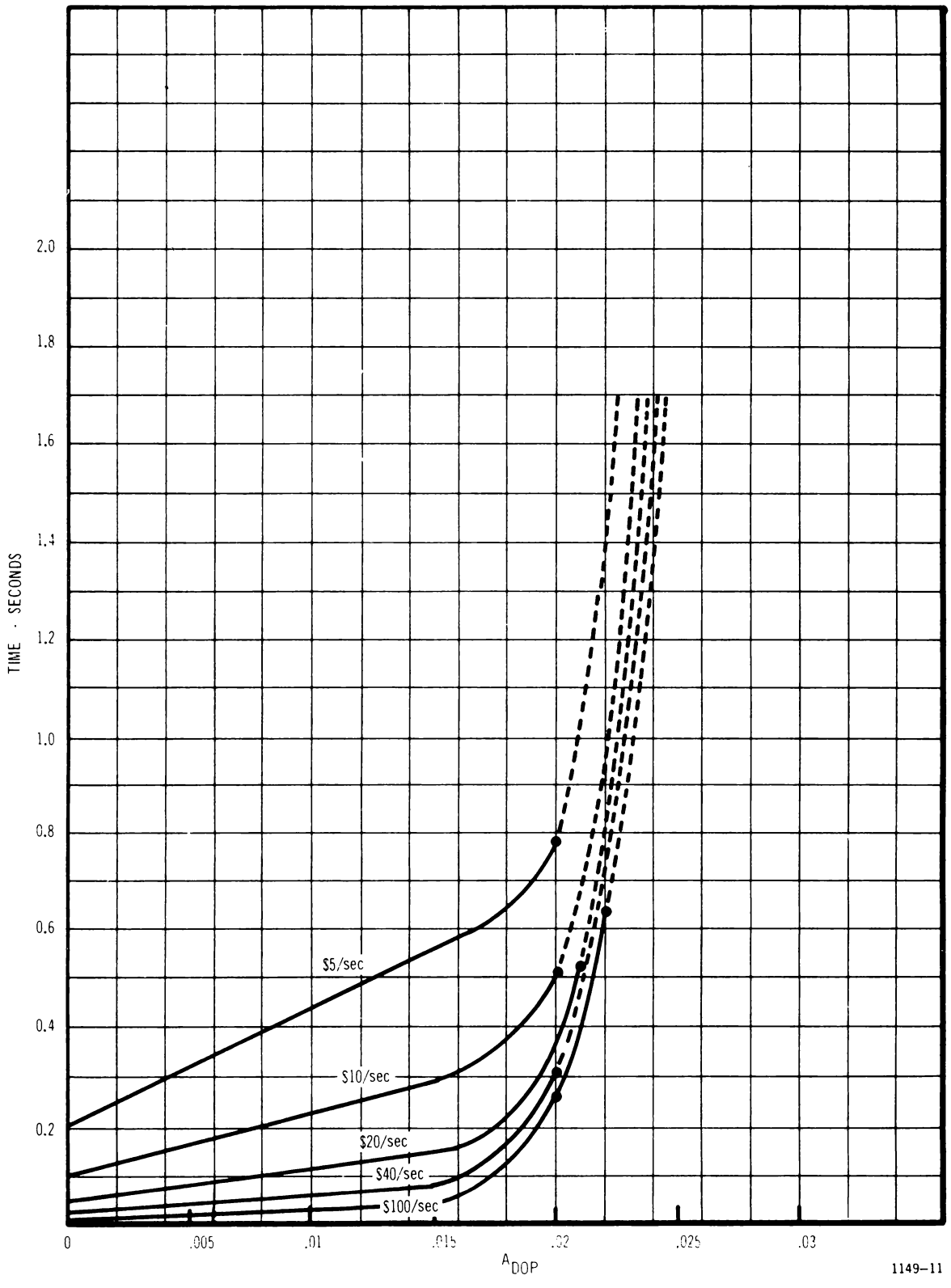

Figure 7-3. Total Reactivity Insertion $3.00

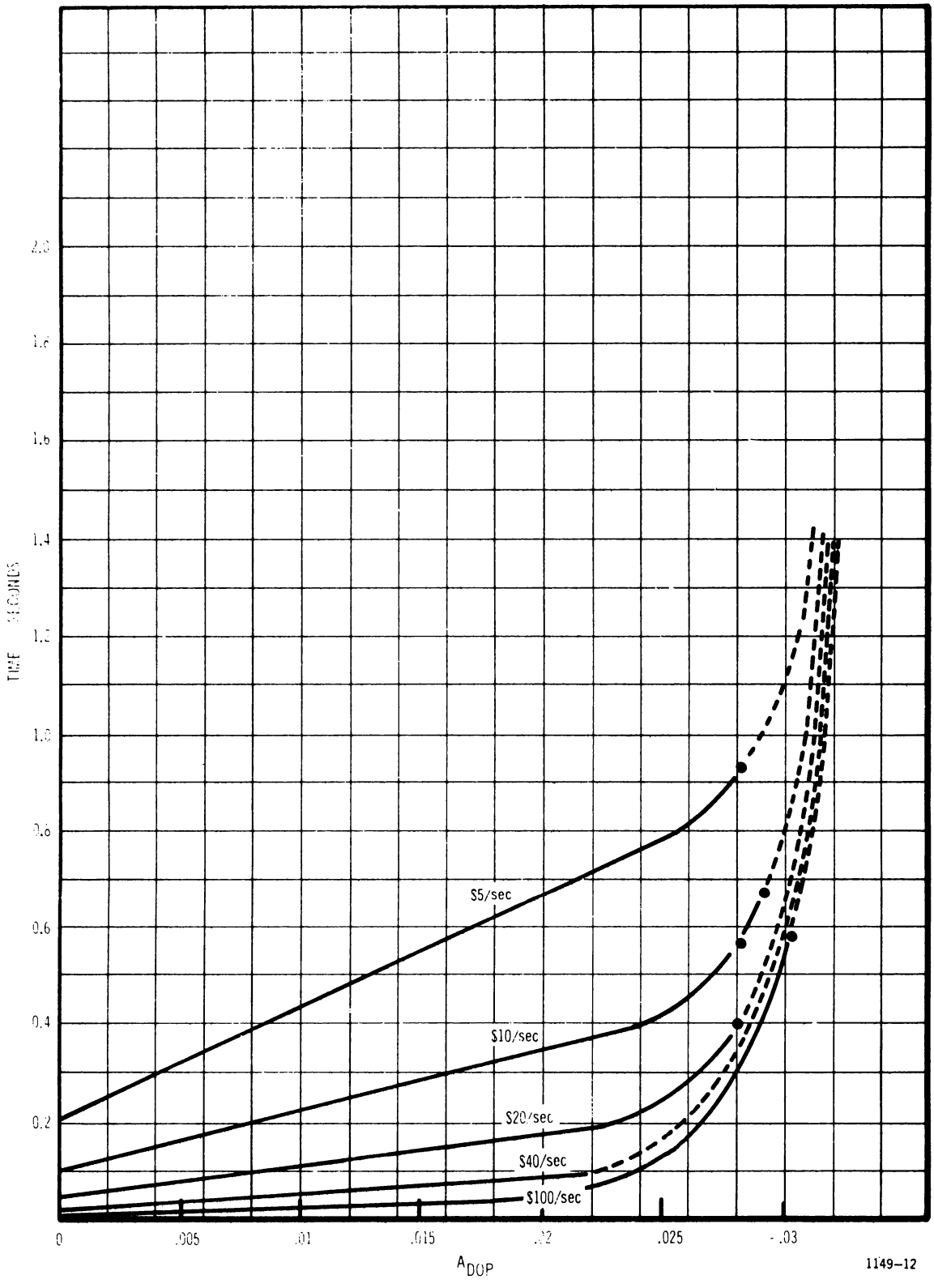

Figure 7-4. Total Reactivity Insertion $4.00

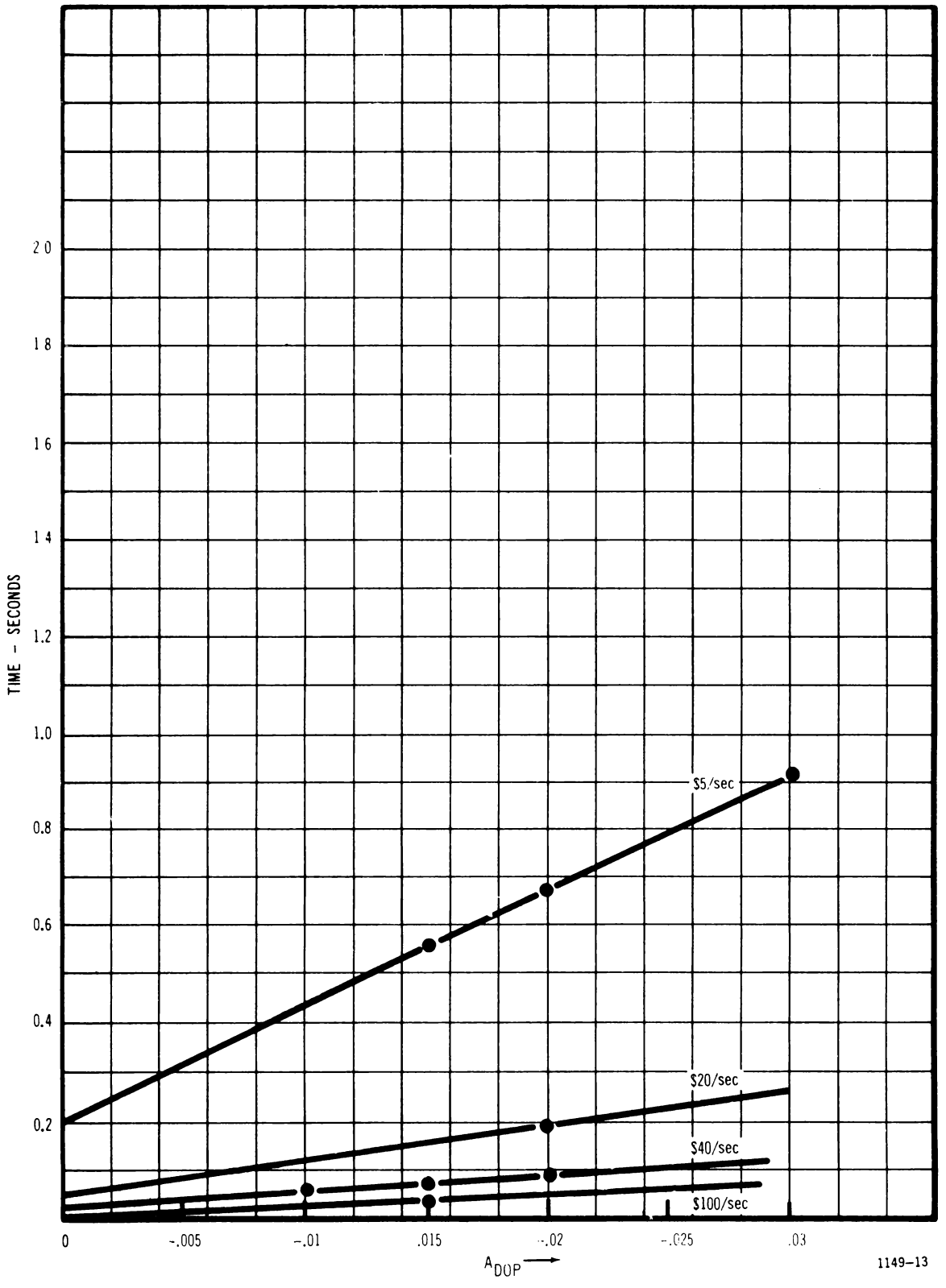

Figure 7-5. Total Reactivity Insertion $5.00

approximately constant for a given design. Thus, if the credible accidental reactivity insertions are established, a combination of detection and control system reaction time, and Doppler coefficient, can be specified such that no core damage will occur.

Calculations will be performed with the FARM computer code to determine the effectiveness of Doppler coefficient in reducing energy release for the uncontrolled accident. The magnitude of the desirable Doppler coefficient in relation to stability will also be examined.

7.2.2 FARM Computer Code

The first version of the FARM (Fast Reactor Meltdown) code is now operational.

7.3 Methods Development

7.3.1 Effect of Level Interference on Pu-239 Cross Sections

The effect of interference between resonances on the Pu-239 cross section in the region of unresolved resonances is presently being investigated using the multilevel formalism of Wigner and Eisenbud.[4,5] The multilevel formalism has been shown to accurately reproduce cross section structure in the very low energy region of resolved resonances, where the single level formalism is inadequate.[6,7,8,9] In order to determine the effect of multilevel methods on the Doppler coefficient of reactivity, two IBM 650 computer codes have been obtained from Phillips Petroleum at NRTS in Idaho. One code (now named MALD after being transferred to the PHILCO 2000) takes discrete resonance parameters (such as fission and reduced neutron widths) at the resonance energies and calculates total and fission cross sections at desired energy points. The code also allows simple calculation of fission resonance integrals. The other code (named TEMP on the PHILCO 2000) Doppler broadens the cross sections obtained from the MALD computer runs. In order to apply the MALD code to the region of unresolved resonances, a sampling routine has been devised, similar to that used in the RAPTURE code,[10] for the fission widths, reduced neutron widths and level spacings.

Calculations of the average zero temperature fission cross section of Pu-239 in the region of unresolved resonances have been performed. For energies of 1000 and 3000 ev, and for an assumed constant level spacing, it was found that the average zero temperature fission cross sections calculated by the multilevel routine agreed with the single level results as computed by the RAPTURE code[10] within three percent for a given state (I, J). Preliminary calculations indicate that the use of a $\nu = 10$ spacing distribution yields larger average cross sections than in the case of a constant spacing. In order to evaluate the effect of multilevel methods on the Doppler coefficient of reactivity for FCR, calculations are being carried out using the TEMP routine in conjunction with the MALD code.

7.3.2 Modification to the MISY Perturbation Routine

The diffusion theory computer code currently used at APED for analysis of fast reactors is called MISY. A modification to the perturbation theory routine in MISY, the PURT module, has been specified. The modification consists of a correction to the treatment of the diffusion coefficient perturbations performed by the PURT routine which takes into account the perturbation of boundary conditions at material interfaces.

7.3.3 Generation of Multigroup Cross Section Files

Programming of the computer code TRAN is underway. TRAN will be used to generate many group elastic and inelastic transfer cross sections for use in EICA. The EICA code will utilize the input from TRAN and other additional input to generate an appropriately averaged set of multigroup cross sections for use in MISY diffusion theory calculations for specific reactor designs. The EICA code has been specified, but programming of EICA has not yet begun.

7.4 References

1. GEAP 4158, Fast Ceramic Reactor Development Program Fifth Quarterly Report October-December 1962.
2. GEAP 4058, Analytical Studies of Transient Effects in Fast Reactor Fuels, by R. B. Osborne, D. B. Sherer, August 1962.
3. GEAP 4130, Experimental Studies of Transient Effects in Fast Reactor Fuels, Series I UO_2 Irradiations, by J. H. Field, November 15, 1962.
4. E. P. Wigner, Physical Review, 70, 606 (1946).
5. E. P. Wigner and L. Eisenbud, Physical Review, 72, 29 (1947).
6. E. Vogt, Physical Review, 112, 203 (1958).
7. M. S. Moore and C. W. Reich, Physical Review, 118, 718 (1960).
8. E. Vogt, Physical Review, 118, 724 (1960).
9. O. D. Simpson and M. S. Moore, Physical Review, 123, 559 (1961).
10. J. H. Ferziger, P. Greebler, M.D. Kelley and J.W.Walton, The RAPTURE Code, GEAP-3923 (July 1962).